Received: 24 March 2025 | Revised: 25 September 2025 | Accepted: 27 September 2025

DOI: 10.1002/esp.70182

RESEARCH ARTICLE

ESPL WILEY

Hot rocks? Divergent rock-surface temperatures during extreme thermal events with implications for physiological stress in rocky shore organisms

Martin A. Coombes

School of Geography and The Environment, University of Oxford, Oxford, UK

Correspondence
Martin A. Coombes, School of Geography and The Environment, University of Oxford, Oxford, UK.
Email: martin.coombes@ouce.ox.ac.uk

Funding information
I am grateful to the support of the British Society for Geomorphology for funding this research (Research Grant BSG-2023-07). This work was also supported by Research England under the Enhancing Research Culture funding stream (via the University of Oxford Social Sciences Division Fixed Term Researcher Fund).

Abstract

While rock–organism thermal interactions on rocky shores have known biogeomorphological relevance, the influences of rock thermal properties on the conditions experienced by rock-dwelling organisms (epiliths) remain understudied. This is a significant gap given the potential ecological and biogeomorphological consequences of changing average and extreme temperatures for coastal ecosystems. Using field block exposure trials in Southern England (including the 2023 September heatwave) alongside laboratory simulations, the thermal responses of four contrasting substrates (limestone, sandstone, basalt and concrete) were compared under the same heating conditions. Indicative organism temperatures were simultaneously obtained using biomimetic sensors (robolimpets [RLs] and robomussels [RMs]) attached to the substrate surfaces. Highly divergent thermal behaviours were observed, with peak substrate surface temperatures ($T_{\max}$) differing by up to 13.2°C (basalt vs. limestone) under heatwave conditions in the field. Relative substrate temperatures were consistent between the field and laboratory ($T_{\max}$ limestone < sandstone < concrete < basalt), corresponding to key material properties such as density and colour; and hotter surfaces were always associated with higher biomimetic temperatures. The degree of association between surface and biomimetic temperatures differed between the two sensor types, attributed to more efficient conductive heat transfer (from substrate to organism) in the case of RLs. Thermal divergence between the two types of sensors was also mediated by rock type, with substrate porosity and evaporative cooling effects having a modulating effect. Biomimetic $T_{\max}$ also diverged under increasingly extreme scenarios depending on the substrates the sensors were attached to. These observations demonstrate how geomorphological approaches can contribute to thermal biology research (hinting at a new 'thermal biogeomorphology'), with implications for patterns of physiological stress, the crossing of critical thermal limits, and resulting changes in the distribution and abundance of geomorphologically relevant species. Key challenges going forward, such as addressing sensor limitations and scale issues, are also identified.

KEYWORDS
biogeomorphology, climate change, heat stress, heatwave, intertidal, physiological stress, rocky shore, thermal biology

---

1 | INTRODUCTION

Very little geomorphological research has been performed on the thermal dynamics of rocky shores, especially in a context of climate change (Mottershead, 2013; Trenhaile, 2014; Viles & Coombes, 2022). This is surprising given the crucial role of temperature (alongside moisture) in rock weathering processes (Robinson & Moses, 2011) and a sustained interest in rocky intertidal biogeomorphology (e.g. Coombes, 2014; Naylor, Coombes, & Viles, 2012; Spencer & Viles, 2002; Trudgill, 1987). At the same time, rising average marine temperatures and more frequent extreme thermal events (i.e. heatwaves; Capotondi et al., 2024; Hobday et al., 2016) are, respectively, linked to chronic and acute thermal stresses in rocky shore species, with widespread impacts on ecological functioning and biodiversity (Hawkins, Burrows, & Mieszkowska, 2023; Helmuth et al., 2006; Meunier, Hacker, & Menge, 2024). In these contexts, the bi-directional energy exchanges between rocky substrates and the organisms that colonise them (epiliths) are of significant interest.

A major challenge is obtaining comparable thermal data for different rock types (and epiliths) when exposed under the same heating conditions. The tradition of thermal simulations in rock weathering research (e.g. McGreevy, 1985; Smith et al., 2005) offers opportunities here. Recently, several researchers have made attempts to incorporate biological variables into laboratory weathering simulations, including seaweed cover (Gowell, Coombes, & Viles, 2015), barnacles (Coombes et al., 2017) and mussels (Baxter, Coombes, & Viles, 2022). This work has revealed intriguing relationships between bio-cover and surface/sub-surface rock thermal regimes that have, so far, only been considered in a context of rock weathering—the implications of rock type, physical properties (e.g. porosity) and divergent thermal behaviours on the conditions experienced by colonising organisms remain significantly underexplored.

After reviewing some of the relevant principles of thermal biology and rock properties (Section 2), experiments used to examine substrate–epilith thermal interactions in the field and laboratory are described (Section 3). These experiments aimed to (1) demonstrate divergent substrate responses under the same heating conditions on natural rocky shores in the UK (including a heatwave event in September 2023) and in the laboratory (Section 4.1); (2) examine the relationships between substrate and indicative organism body temperatures using 'biomimetic' sensors (Section 4.2); (3) explore the potential mediating influence of substrate porosity and evaporative cooling (Section 4.3); (4) assess responses under increasingly extreme (simulated) heatwave conditions (Section 4.4); and (5) consider the implications for thermal biology in a warming climate (Section 4.5). Lastly, some directions for future research in 'thermal biogeomorphology' are discussed in Section 5.

2 | LITERATURE REVIEW

2.1 | Climate change and extreme thermal events on rocky shores

Mass mortality events caused by exposure to lethal (sustained and extreme) high temperatures during heatwaves are known to occur on rocky shores (Garrabou et al., 2009; Harley, 2008; Tsuchiya, 1983) and are expected to increase under future climate scenarios (Hobday et al., 2023; Wernberg et al., 2013). At the same time, sub-lethal but recurrent physiological stress, especially leading up to a heatwave event, can modulate critical thermal thresholds (King et al., 2025) and drive changes in fitness (Beukema, Dekker, & Jansen, 2009; Seuront et al., 2019). Alongside direct biodiversity loss, these effects are linked to broad-scale biogeographic reorganisation and regime shifts in the coastal zone, often involving foundation species (e.g. macroalgae, seagrass and corals; Harley et al., 2006; Hawkins, Burrows, & Mieszkowska, 2023; Ishida et al., 2023; Mieszkowska et al., 2021), with broader implications for ecosystem service provision and other socioeconomic impacts (Smale et al., 2019; Smith et al., 2021). Better understanding the factors influencing such sub-lethal and lethal thermal stresses is, therefore, needed so that vulnerability and resilience to climate change can be predicted at individual, community and ecosystem scales (Denny, Miller, & Harley, 2006; Kordas et al., 2015; Mislan, Wethey, & Helmuth, 2009; Smale & Wernberg, 2013).

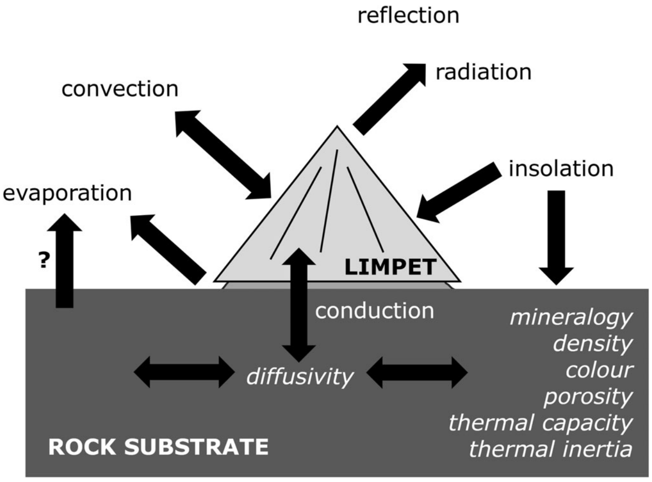

FIGURE 1 Schematic representation of heat transfers affecting epilithic organisms during aerial exposure on rocky shores. In the context of this study, heat transfers between the surface and epiliths occur via conduction, which can vary depending on substrate type. Cooling of organisms via evaporation (as a source of latent heat) is widely acknowledged, yet evaporative cooling of the substrate is not typically considered. Relevant rock properties are shown in italics. Adapted from Denny and Harley (2006) and Seuront, Ng and Lathlean (2018).

Epilithic invertebrates such as limpets, barnacles and mussels, which live on the surfaces of rocky substrates, are marine ectotherms exposed to terrestrial conditions at low tide. This imposes strict stress gradients via organism physiological tolerances to heat and desiccation that give rise to characteristic vertical zonation (Paine & Levin, 1981). During a tide cycle, epiliths are exposed to dramatic changes in temperature that often exceed 20°C or more (Helmuth, 1999), especially in temperate regions where tidal ranges are large and aerial exposure can last several hours at a time (Sarà, Kearney, & Helmuth, 2011). Organism body temperatures fluctuate in response to these variable conditions (Davison & Pearson, 1996; Harley & Helmuth, 2003; Helmuth, 1998; Lathlean, Seuront, & Ng, 2017; Wethey, 2002). Consequently, species in the upper intertidal zone live close to their physiological limits (Porter & Gates, 1969; Somero, 2002), making them particularly vulnerable to shifts in thermal regimes. These conditions offer ideal model systems to study the influence of changing abiotic conditions on physiology and ecology (Hawkins, Burrows, & Mieszkowska, 2023).

2.2 | Thermal biology, microclimates and biomimetic sensors

Field temperature data collected over long timescales and large spatial scales poorly predict the microclimatic conditions experienced by individual organisms on rocky shores. To help tackle this scale challenge, pioneering modelling work in the late 1990s (Helmuth, 1998, 1999) reinvigorated research on the vulnerability of intertidal communities to climate change (Helmuth, 2002; Helmuth et al., 2006; Kearney et al., 2010; Lathlean et al., 2017; Lathlean, Ayre, & Minchinton, 2013; Petes, Menge, & Harris, 2008). This work shows that heat budget models are most accurate only when a wide range of parameters are included (solar flux, wind speed, ground temperature and so on), which control conductive, convective and radiative heat transfers (Figure 1; Denny & Harley, 2006; Helmuth, 1998; Sarà, Kearney, & Helmuth, 2011). This need for model complexity reflects the fact that local factors (e.g. shading effects, wind, local water retention and ground temperature) are more important controls on spatial patterns of physiological stress than latitudinal gradients (Finke, Navarrete, & Bozinovic, 2007; Pearson, Lago-Leston, & Mota, 2009). There is, therefore, a recognised need for continued improvement in understanding of the full range of factors affecting organismal thermal budgets (Dong, 2023).

In addition to thermal modelling, the development of miniaturised and robust 'biomimetic' data loggers has been a significant methodological advance. By mimicking the size, shape and colour of marine animals, these sensors record temperatures that, despite some limitations (see Section 5), are much more representative of living organisms than simple measures of air temperature and relative humidity (Mitchell et al., 2024). Examples include so-called 'robolimpets (RLs)', 'robomussels (RMs)', 'robobarnacles' and 3-D printed 'EnvLoggers' (Chan et al., 2016; Helmuth et al., 2016; Judge, Choi, & Helmuth, 2018; Lima & Wethey, 2009). Given their robustness and relatively low cost, biomimetic sensors have allowed more accurate and representative data collection for input and calibration of thermal models, as well as more geographically widespread monitoring of climate change impacts on marine epiliths (Reese, 2023). In contrast, to my knowledge, biomimetic sensors have never been applied in biogeomorphological research.

2.3 | The substratum contribution

Weathering research has shown how a range of physical rock properties (porosity, surface roughness, thermal capacity, thermal conductivity, colour and so forth) are linked to complex thermal behaviours (e.g. Hall & Thorn, 2014; McGreevy, 1985; Warke, Smith, & Magee, 1996). In ecological research, Rejmánek (1971) recognised that rock type and rock properties (such as lithology) are important thermal mediators in ecosystems, referring to potentially 'heat efficient rocks' like basalt, which store heat. Raimondi (1988) attributed differences in zonation between two rocky shores in the Gulf of California to rock colour and thermal capacity, and in a rare study, Janetzki, Benkendorff and Fairweather (2021) linked the minerology and lithology of six intertidal boulders to spatially variable thermal behaviours and habitat conditions. Along with field data, thermal models demonstrate the critical importance of the substratum, which typically reaches temperatures substantially hotter (or colder) than the air. Indicatively, substratum ('ground') temperature is generally considered a good proxy for organismal body temperatures on rocky shores (Helmuth, 1998; Mitchell et al., 2024).

Despite its known importance, Cryan et al. (2021) note that substratum thermal properties remain a relatively unexplored component of heat exchange in intertidal systems. There is, for example, a lack of data for different rock types, especially given the range of lithologies characterising the world's coastlines (Kennedy, Stephenson, & Naylor, 2014). The evaporative behaviours of biological substrates (and associated cooling effects) also remain largely unexplored in the intertidal zone. Simple experiments using simulated tidal conditions have revealed a complex dynamic interplay between rock thermal and moisture (hygro) dynamics (Coombes & Naylor, 2012), with evidence that these processes might mediate rock-surface microclimates to some extent (Coombes, 2011; Coombes et al., 2017). In addition to moderating hygro-thermal weathering processes on rocky shores, these effects may also have biogeomorphological relevance by influencing the current and future distribution and abundance of bioeroders and bioprotectors (Coombes, 2014; Naylor, Coombes, & Viles, 2012; Naylor, Viles, & Carter, 2002; Spencer & Viles, 2002). To better understand this potential, this study aimed to evaluate the influence of substrate type on the temperatures experienced by colonising organisms in the context of climate change and extreme thermal events on rocky shores.

3 | METHODOLOGY AND METHODS

Using a combination of field exposure trials in Southern England and laboratory simulation in an environmental chamber, the surface temperatures of four contrasting substrates (limestone, sandstone, basalt and concrete) were measured along with concurrent indicative organism temperatures using biomimetic sensors. These datasets were compared to evaluate rock–organism thermal relationships between (a) substrate types, (b) organism (sensor) types and (c) simulated heatwave events of differing magnitude.

3.1 | Substrates

Limestone, sandstone, basalt and concrete were prepared as experimental blocks (100 × 100 × 50 mm); the rock blocks were cut from larger pre-existing samples, and the concrete was cut from a commercial paving slab. Given the diversity of coastal lithologies around the UK and elsewhere, as well as the common use of concrete in coastal engineering, these materials were chosen to represent a range of contrasting substrate types and properties (colour, density, porosity and so forth; Table 1). The size of the blocks was a compromise between portability—especially in the field—and thermal mass. Although the size of a rock mass (e.g. a single block vs. a shore platform) undoubtedly affects thermal properties (Gedan et al., 2011), the relative comparison between substrate types was central to this study, which

TABLE 1 Summary of substrate types used in field and laboratory block (100 × 100 × 50 mm) exposure experiments.

	Description	Density (kg/m^3)	Porosity[a] (%)	Dry colour[b,d] (L^*,a^*,b^*)	Wet colour[c,d] (L^*,a^*,b^*)	Darkening when wet (wet L^* vs. dry L^*, %)
Limestone	Portland, England: Jordans Basebed, well-sorted oosparite limestone.	2286.92	18.34	75.9,2.1,13.2 (albedo = 0.79)	65.2,3.7,16.9 (albedo = 0.60)	15.2
Sandstone	Locharbriggs, Scotland: medium-grained Permian red sandstone.	2034.84	19.37	51.9,11.6,15.4 (albedo = 0.53)	33.8,12.4,13.8 (albedo = 0.35)	42.4
Basalt	China: fine-grained, dense and olivine bearing.	3012.44	1.30	49.6,−0.8,1.5 (albedo = 0.51)	27.7,−0.3,1.2 (albedo = 0.18)	56.6
Concrete	Commercial paving slab: Cement and aggregate unknown.	2034.78	12.45	72.3,−0.2,6.6 (albedo = 0.76)	60.6,−0.2,7.0 (albedo = 0.55)	17.6

[a] Porosity (%) was determined as saturated pore volume/total volume × 100.

[b] Blocks were oven-dried at 60°C for 24 h.

[c] Blocks were saturated at room temperature for 48 h.

[d] Colour was determined using a CM-700d spectrophotometer (Konica Minolta, Japan), where L^* indicates darkness from 0 (black) to 100 (white); a^* indicates red/green, with positive values indicating red and negative values indicating green; and b^* indicates blue/yellow, with positive values indicating yellow and negative values indicating blue (mean, $n = 3$). Albedo values are indicative only, derived using (1) a normalised model of lightness (L^*/100) and incorporating (2) nonlinear correction based on measured reflectance curves for natural surfaces and (3) material-specific adjustments (Bowker et al., 1985).

remains valid given that all blocks had the same dimensions. Similarly, although cut surfaces are unrepresentative of most natural surfaces (see Section 5), this ensured that differences could be attributed to inherent rock properties rather than surface complexity (e.g. Meager, Schlacher, & Green, 2011).

A 3-mm-diameter hole was drilled into the underside of each block, in the centre, to accommodate flexible and waterproof thermistor probes (PB-5009-0 M6, Gemini Data Loggers; accuracy = 0.2°C between 0 and 70°C), attached to dual-channel Tinytag dataloggers (TGP-4520, Gemini Data Loggers). When inserted, the probes were positioned 1 cm below the upper 'colonised' surfaces of the blocks and recorded indicative surface temperatures at 1 min intervals during the experiments. The blocks were also coated in three coats of polyurethane varnish on all except the upper 'colonised' surface to restrict moisture exchange to this one face (e.g. Smith & McGreevy, 1983), thereby better reflecting water uptake and evaporation from shore platform surfaces (Coombes et al., 2017). Substrate surface temperature data were downloaded from the Tinytag probes inserted into each block using Tinytag Explorer software (Gemini Data Loggers).

3.2 | Biomimetic sensors

Temperature dataloggers (EnvLoggers, T2.4) manufactured by ElectricBlue were used to obtain indicative organismal body temperatures. The EnvLogger system comprises a miniaturised, fully waterproof temperature logger and a companion smartphone app. Two types of biomimetic EnvLoggers were used: RLs (40 × 48 mm at the base, 20-mm height, light grey), designed to mimic medium-sized *Patella* individuals, and 'RMs' (30 × 60 × 12 mm, black) designed to mimic adult *Mytilus* individuals. Both mussels and limpets are found globally, with these particular species common across European shorelines, including in Southern England. Prior to the experiments, all sensors were calibrated at 20 and 40°C using an environmental chamber, with the differences across both groups <0.5°C.

During the field exposures and laboratory simulations (see the following sections), both types of EnvLogger (RLs and RMs) were set to record temperature at 1 min intervals at a resolution of 0.1°C. One of each sensor type was attached, side-by-side, to the centre of each exposure block (Figure 2). To achieve representative attachment, the RLs were attached using a thermally conductive paste (Thermalright TF4, Taiwan), aiming to simulate the direct contact between the tissues of limpets and their substrates. Care was taken to use the same amount of paste in each case. The RMs were attached using a small ball of putty, which allowed the 'shells' to be positioned on their long edge, with the ventral side attached to the substrate and the dorsal side facing up, thus mimicking living individuals in the field (Figure 2a, lower panel). The RLs remained attached to the blocks for the duration of the study, whereas the RMs were easily removed and reattached as needed during the experiments. The EnvLogger mobile app (installed on a Samsung Galaxy S21) was used to download data directly from the sensors at the end of each exposure/simulation using near-field communication. Raw datasets were imported, collated and checked using Microsoft Excel v.2411.

3.3 | Field exposure trials

The four sample blocks, with biomimetic sensors attached, were exposed in the field under conditions ranging from 'warm' to 'heatwave' during the summer of 2023. Exposures were made in the following three locations using the same blocks: (1) a chalk (Seaford Chalk Formation, Cretaceous age) rocky shore platform at Hope Gap, East Sussex (three low-tide exposures in July 2023); (2) a slate (Mylor Slate Formation, Late Devonian age) shore platform at Mousehole, Cornwall (one low-tide exposure in August 2023); and (3) a suburban garden in Kidlington, Oxfordshire (two exposures in September 2023) (Table 2). The first two sites are representative of intertidal environments on the south coast of England, and the latter site was opportunistically included to take advantage of a significant and unusually late summer heatwave (4–10 September 2023). This heatwave produced the warmest September days on record in the UK, with air temperatures exceeding 30°C on seven consecutive days across southeast England, with anomalies of > 12°C relative to the 1991–2020 average (Kendon, 2023).

At the two rocky shore sites, the blocks were exposed between the mean and high-water neap tide levels during low-tide periods,

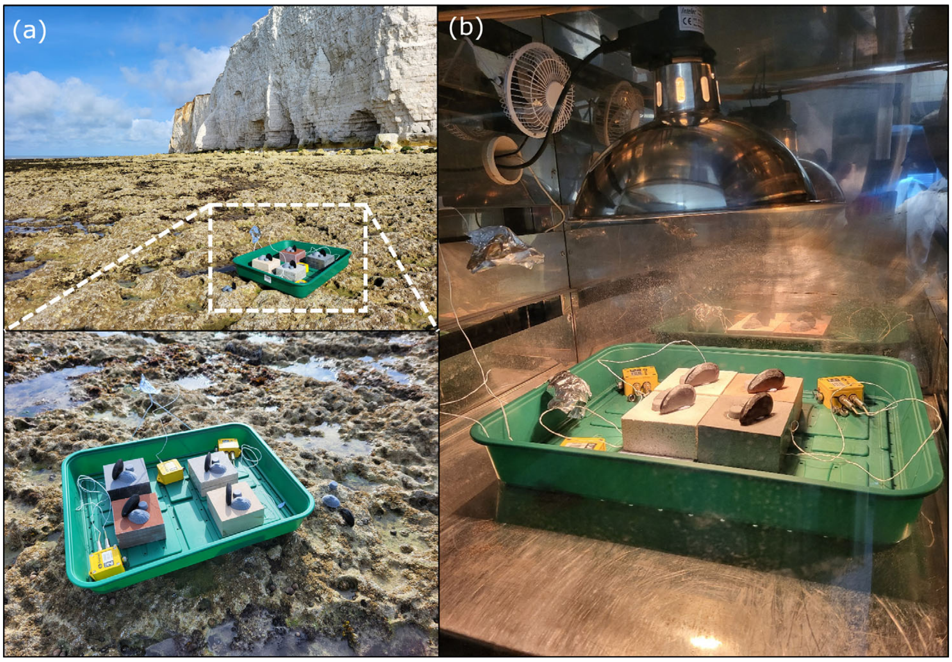

FIGURE 2 Data collection setup: (a) Field exposure on a shore platform at Hope Gap, East Sussex, England, with heating from the sun; (b) laboratory simulation in an environmental chamber with heating from an infrared lamp (250 W with a 50% reducer switch). In all cases, four substrates (limestone, sandstone, basalt and concrete) were exposed with biomimetic sensors (EnvLoggers, T2.4; robolimpets and robomussels) attached to their surfaces. Regular round EnvLoggers were also attached for comparison (data not shown).

TABLE 2 Experimental field exposures of different rocky substrates and biomimetic sensors.

#	Location	Date	Setting	Time of exposure	Weather conditions	Peak air temp (shade)
1	Hope Gap, East Sussex, UK	18-07-23	Shore platform	8:15–12:15	Still air, patchy slow-moving cloud	25.2°C
2	Hope Gap, East Sussex, UK	19-07-23	Shore platform	09:00–13:00	Still air, patchy slow-moving cloud	31.1°C
3	Hope Gap, East Sussex, UK	20-07-23	Shore platform	09:00–13:00	Light breeze, patchy slow-moving cloud	24.4°C
4	Mousehole Harbour, Cornwall, UK	09-08-23	Shore platform	12:30–16:30	Moderate breeze, overcast	28.0°C
5	Kidlington, Oxfordshire, UK	07-09-23	Garden	11:30–15:30	Still air, clear sky	33.8°C
6	Kidlington, Oxfordshire, UK	08-09-23	Garden	12:00–16:00	Light breeze, clear sky	33.1°C

placed in position for at least 4 h and collected ahead of the incoming tide. Before each exposure, the blocks were soaked in water overnight to better simulate saturated intertidal rock. The soaked blocks (and sensors) were then wrapped in wet paper towel for transport to site to minimise evaporation before exposure. On site, all of the blocks and sensors were immersed in a rock pool for approximately 15 min prior to exposure to equilibrate with the temperature of the seawater. At the start of each exposure period, the Tinytag probes were inserted into each block and secured, and the RMs were attached alongside the RLs as described in Section 3.2. The blocks and loggers were positioned horizontally on the platforms, in a plastic tray, and an additional Tinytag probe (shaded with foil) was secured 30 cm above to record air temperature (Figure 2b). At the garden site, the same procedure was followed except that the samples were positioned on a low table, in an unshaded position, and the sensors were plunged into cool water rather than a tide pool before exposure to the sun.

3.4 | Laboratory simulations

The same set-up as used in the field was replicated under laboratory conditions, inside an environmental chamber (SANYO–FE 300H). A 250 W infrared (IR) thermal lamp (Intelec™ 630105) was secured inside the chamber to simulate insolation (e.g. Coombes, 2011; Coombes et al., 2017; Gowell, Coombes, & Viles, 2015). Based on pilot testing, the IR bulb produced unrealistic temperatures in the chamber when used at full power. Therefore, a 50% reducer switch was used (approximately 125 W), which produced more satisfactory conditions.

Each simulation first involved placing the tray containing the blocks and attached sensors into the chamber for approximately 30 min at a pre-heated temperature of 15°C (with the lamp off). This was carried out to equilibrate all the materials and sensors to a temperature approximating the sea surface in summer along the southern coast of England. At the start of each run proper, the IR lamp was switched on and the chamber switched to the target temperature and left for a period of 4 h (Figure 2b). Each run simulated a single 'low-tide event' with clear-sky conditions during the middle of the day, when the sun is highest in the sky. Three sets of experiments were run, each replicated twice, with direct heating from the lamp and air temperature in the chamber held at 20, 30 or 40°C. These temperatures were chosen to broadly reflect current and future summertime/heatwave conditions in southern England. Air temperature inside the chamber was continuously recorded using a shaded Tinytag probe secured 30 cm above the surfaces of blocks, as in the field exposures (Figure 2). Each simulation was repeated under both dry (with dry blocks) and wet (with saturated blocks) conditions to isolate evaporative cooling effects. Block weights before and after each (wet) simulation were recorded as a simple measure of evaporative loss. For simplicity, relative humidity (RH) was not controlled but was allowed to vary within the chamber; RH ranged between 60% and 90% during the wet simulations, broadly reflecting conditions occurring on still, summer days on rocky shores in southern England (e.g. Coombes et al., 2017).

In total, 12 simulations were run in the laboratory—two simulations at each temperature (20, 30 or 40°C)—under both 'dry' and 'wet' conditions.

3.5 | Data analysis

Temperature maxima (T_{max}) values were calculated for the air, substrates and two types of sensors (RMs and RLs) for each of the field exposures ($n = 6$) and laboratory simulations ($n = 12$). Peak temperatures are of relevance for thermal biology given threshold-driven critical thermal limits in most species (e.g. Harley et al., 2009). To better isolate the influences of substrate type, and to minimise collinearity effects, T_{max} data were also normalised to correct for air temperature. This involved subtracting air T_{max} values from the corresponding substrate/sensor T_{max} values (referred to as $T_{max\text{-}air}$). When comparing field and laboratory data, only relative trends between substrate and logger types were considered, rather than absolute values, owing to uncontrollable factors such as time of day and insolation angle (Table 2; see Section 4.2).

The factors explaining surface and biomimetic $T_{max\text{-}air}$ were assessed using stepwise (forward selection) multiple linear regression, with predictor variables included or excluded from the models based on the F-test and using a set threshold of $p < 0.05$ to avoid overfitting. Where appropriate, substrate type was included as a categorical predictor variable using dummy coding (Suits, 1957). In all cases, normal probability and residuals plots were used to confirm normality and homoscedasticity. Collinearity between predictor variables was assessed using the variable inflation factor (*VIF*). Relative differences and overall trends between the dry and wet simulations and across the three laboratory scenarios (20, 30 and 40°C) were compared using standard graphical plots produced in Microsoft Excel v.2411.

4 | RESULTS AND DISCUSSION

This section presents and discusses the results by focussing on divergent substrate temperatures (Section 4.1), relationships between surface and biomimetic temperatures (Section 4.2), moisture effects (Section 4.3), responses under different event magnitudes (Section 4.4), and finally, implications for the thermal biology of rocky shores (Section 4.5).

4.1 | Different substrates show divergent surface temperatures under the same heating conditions

The overall patterns of warming recorded in the field reflect different times of exposure during the day. The substrates and sensors showed a gradual warming trend when exposed during morning low tides, when the air was still cool and the sun was low in the sky (e.g. Hope Gap, Figure 3a). This contrasted with very rapid heating in response to afternoon exposure, when the air was already hot and (on clear days) insolation was at its peak (e.g. Kidlington, Figure 3b). Overcast conditions at one of the sites (Mousehole, Figure 3c) resulted in notably muted rates and magnitudes of warming, even during the afternoon when the air was relatively warm. The shorter-term and lower-magnitude fluctuations in temperature recorded during the field exposures (compare field data in Figure 3 with simulation data in Figure 5) are attributed to variable insolation under passing cloud (Coombes, 2011) as well as other local-scale factors, such as low-level air movements that facilitate convective heat transfers (Seuront, Ng, & Lathlean, 2018).

The different substrates showed highly divergent thermal behaviours in the field (Figure 4). In all cases, basalt attained the highest T_{max} while limestone remained coolest; concrete and sandstone attained similar values, although concrete tended to peak higher on warmer days (Figure 4 and Table 3). The anomalous 'cool' event in Figure 4 corresponds to the hot but overcast day at Mousehole (9 August 2023), when direct solar heating of the blocks and sensors was prevented by cloud. Of note, the range of T_{max} values across the four substrates was much lower on this overcast day, contrasting with greater divergence under clear-sky conditions. Across all six field exposures, the average peak surface temperature above air ($T_{max\text{-}air}$) for limestone, sandstone, concrete, and basalt was 1.3 ± 2.6, 3.9 ± 3.3, 4.5 ± 3.9 and 11.0 ± 5.6°C, respectively. The maximum difference was recorded during the September heatwave (7 September 2023), when the surface temperature of basalt peaked above 50°C and 16.9°C above the air (Figure 4). A comparable difference of 17.5°C was recorded between basalt and air in the 30°C (wet) simulation.

Regression analysis of the field data showed that air temperature (T_{max}) alone explained 58% of the variation in surface T_{max}, irrespective of substrate type ($R^2 = 0.58$, $F[1,22] = 30.11$, $p < 0.001$, SE = 4.8°C). When substrate type was included as a variable set, the predictive power of the model increased to 80% (Table S1). Across all the substrates, a 1°C increase in peak air temperature corresponded to an average 1.5°C increase in surface T_{max}. However, under the same exposure conditions, relative to limestone as the coolest substrate overall, sandstone T_{max} averaged 2.6°C higher, concrete 3.1°C higher and basalt 9.6°C higher. Therefore, while peak air temperature was a good overall predictor of surface T_{max}, substrate type was an important mediator.

In the laboratory simulations, in which heating was always directly from above, temperature changes corresponded well to the afternoon field exposures under clear-sky conditions (compare simulated data in Figure 5 with field data in Figure 3c). Based on the wet simulations,

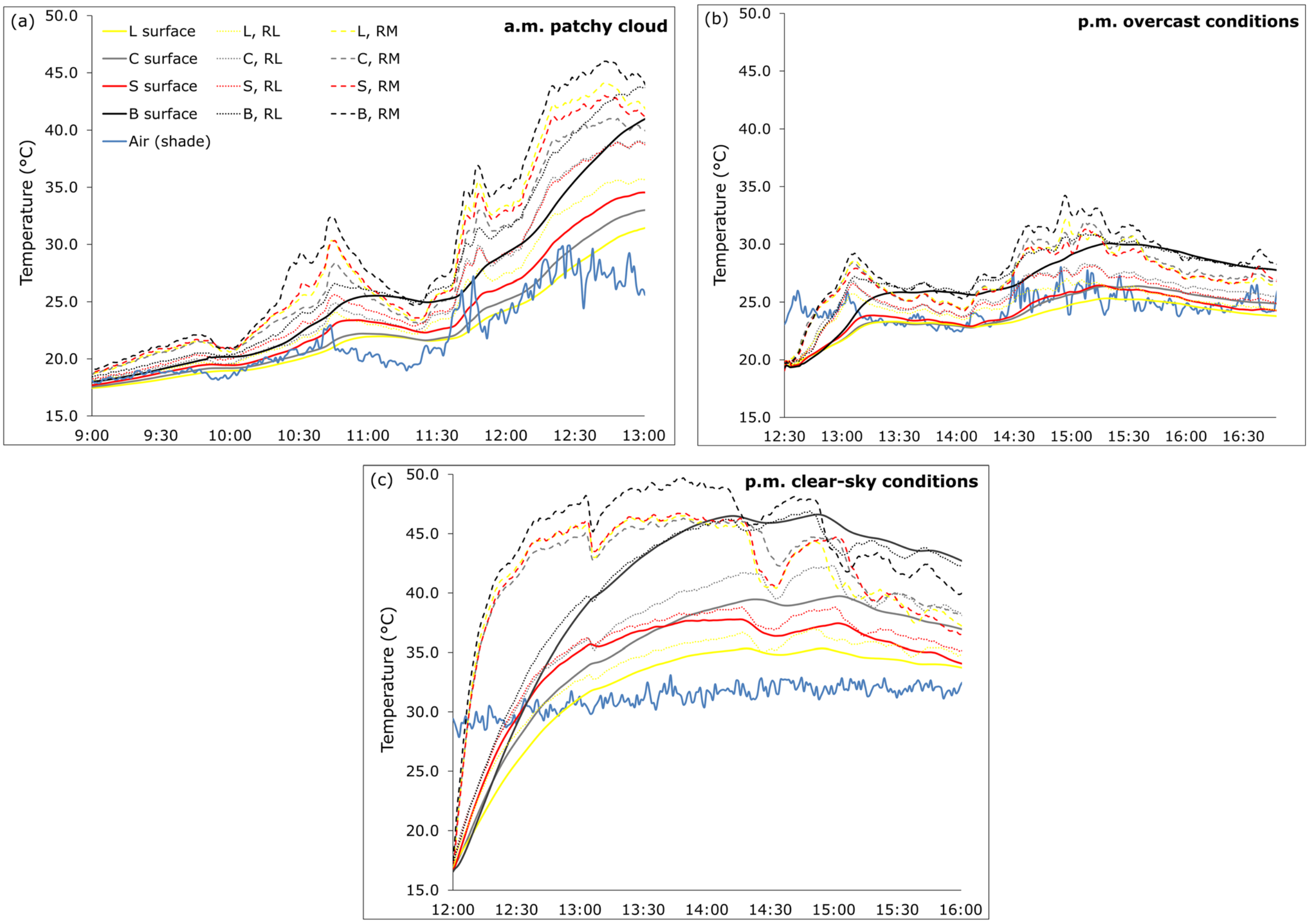

FIGURE 3 Example temperature time-series plots obtained using the same experimental setup at (a) Hope Gap, East Sussex, 19-07-23 (air $T_{\max} = 31.1°\mathrm{C}$, patchy slow-moving cloud, morning exposure); (b) Mousehole, Cornwall, 09-08-23 (air $T_{\max} = 28.0°\mathrm{C}$, overcast, afternoon exposure); and (c) Kidlington, Oxfordshire, 08-09-23 (air $T_{\max} = 33.1°\mathrm{C}$, clear-sky conditions in the afternoon during an official heatwave). L = limestone, C = concrete, S = sandstone, B = basalt. RL = robolimpet, RM = robomussel.

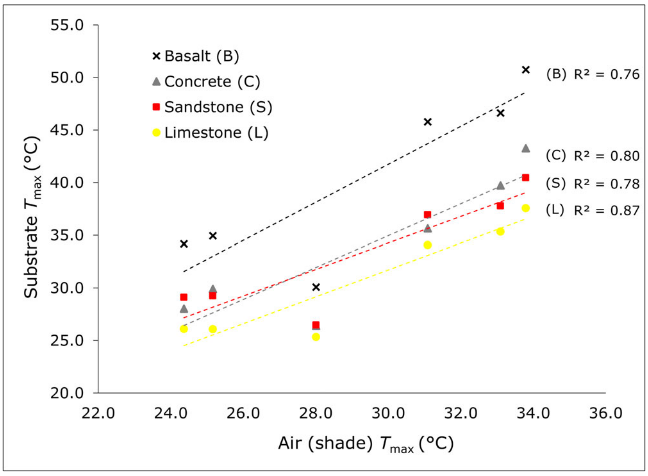

FIGURE 4 Maximum temperatures ($T_{\max}$) of four substrates across six field exposures. Data represent clear-sky or light cloud conditions in all but the anomalous event at Mousehole (air $T_{\max} = 28.0°\mathrm{C}$), when conditions were hot but overcast.

which better replicate field conditions, a significant divergence in $T_{\max}$ between the substrates (ANOVA $F[3,20] = 40.02$, $p < 0.001$) was consistent with the field results; basalt peaked at higher temperatures, limestone remained coolest, and sandstone and concrete peaked somewhere between the two (Table 3 and Figure 5b). Compared to the dry simulation, the difference in $T_{\max}$ between sandstone and concrete was notably enhanced in the wet simulation (Figure 5), which can be explained by the relative evaporative cooling efficiency of the porous sandstone, especially during the later stages of the simulations (see Section 4.3).

Thermal divergence between substrates exposed under the same heating conditions is not unexpected, if rarely reported. Materials with lower specific heat capacity—indicating the amount of heat energy required to raise the temperature by a fixed amount—heat up relatively quickly. For basalt, which has a low specific heat capacity and high solar absorptance (dark in colour), density, and thermal conductivity, higher peak temperatures were reached relative to the other materials (Xiong et al., 2020). In contrast, rocks with higher solar reflectivity (light colour) and specific heat capacity, including limestone and sandstone (Table 1), heat more slowly, remaining relatively cool when exposed to the same heating regime.

Rejmánek (1971) concluded that under comparable conditions, igneous rocks including basalt are predisposed to higher surface temperatures; Marshall, McQuaid and Williams (2010) found that lighter-coloured sandstone remained cooler than darker sandstone on a seawall in Brunei Darussalam; and Judge, Botton and Hamilton (2011) recorded hotter temperatures on 'black rock' compared to 'white rock' in the supralittoral fringe of St John, United States Virgin

TABLE 3 Indicative maximum temperature (T_{max}) ranges of different substrates across six field exposures and six laboratory (wet and dry) simulations.

	Surface T_{max} range[a]		
	Field exposures ($n = 6$, °C)	Wet simulations ($n = 6$, °C)	Dry simulations ($n = 6$, °C)
Air (shade)	24.4–33.8	20.0–40.0	20.0–40.0
Limestone	26.1–34.1	26.5–44.4	29.5–51.5
Sandstone	26.5–40.4	26.7–44.5	34.5–55.3
Concrete	26.7–43.2	32.6–52.5	34.1–56.0
Basalt	30.1–50.7	37.3–56.9	36.4–61.0

[a]Note that differences between the range of temperatures occurring in the field and those simulated in the laboratory (top row) mean that comparisons of absolute values should be avoided. Relative comparisons between substrates remain valid and are consistent between all sets of experiments.

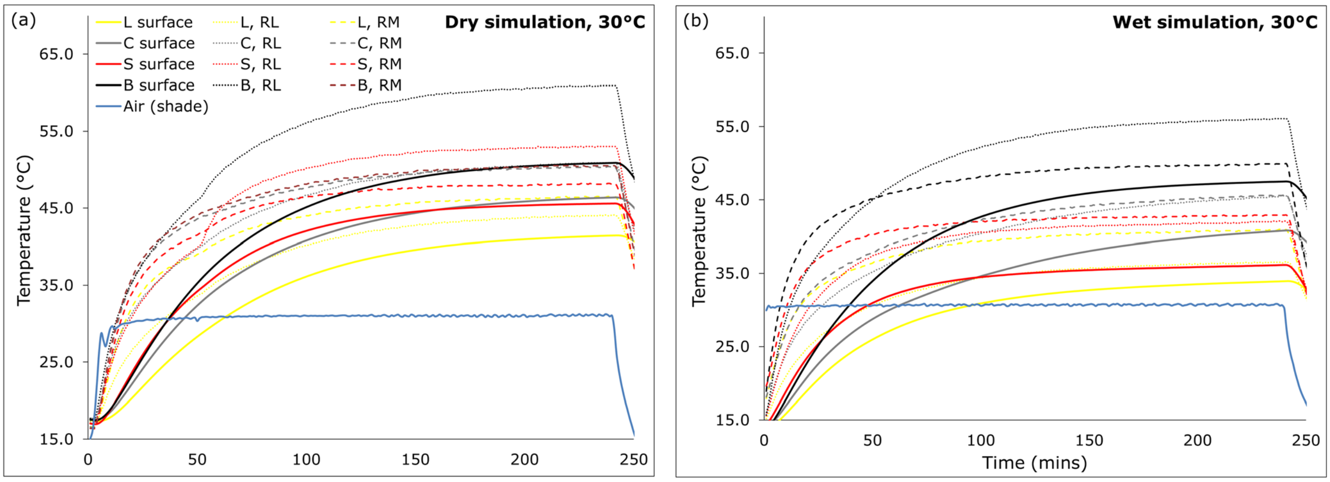

FIGURE 5 Example temperature time-series plots obtained from laboratory simulations using the same setup as in the field (see Figure 3) under a 30°C air temperature scenario with (a) dry and (b) wet sample blocks and attached biomimetic sensors. L = limestone, C = concrete, S = sandstone, B = basalt. RL = robolimpet, RM = robomussel.

Islands. Along the Fleurieu Peninsula of South Australia, Janetzki, Benkendorff and Fairweather (2021) also reported that lighter-coloured limestone and quartzite were cooler than darker siltstones, with the greatest recorded difference under the same heating conditions being 10.2°C. In this study, the greatest difference in surface temperature in the field (13.2°C) occurred between the relatively light limestone and dark basalt during the September heatwave. In comparison to limestone, the darker sandstone also consistently attained higher T_{max} values in the field despite having a lower density more typical of rocks with higher heat capacity (Tables 1 and 3). In the laboratory, the tendency for sandstone to peak higher than limestone was observed in the dry simulations, but this was less clear in the wet simulation (Table 3). This might reflect complex and dynamic changes in colour (and heat absorption properties) during exposure, especially in the case of sandstone, which, relative to the dry state, was 42.4% darker when wet compared to 15.2% darker in the case of limestone (Table 1).

Overall, both the field and laboratory simulations demonstrated the highly divergent thermal behaviours of the different substrates, with patterns of surface warming and relative magnitudes of heating determined by a combination of thermally relevant material properties (i.e. density and colour) and heating conditions (i.e. time of exposure and cloud cover). Alongside the important control of air temperature, substrate type was significant in explaining the measured variability in peak surface temperatures during warm summertime and heatwave conditions in southern England.

4.2 | Substrate modulates relationships between surface and biomimetic temperatures

In the field, the hotter a surface was relative to the air ($T_{max\text{-}air}$), the higher the corresponding temperature peaks of the biomimetic sensors attached to it (Figure 6). As a predictive relationship, this was notably stronger for RLs ($R^2 = 0.89$, $F[1,22] = 175.33$, $p < 0.001$, SE = 1.85°C) than for RMs ($R^2 = 0.51$, $F[1,22] = 23.25$, $p < 0.001$, SE = 2.86°C), although both were statistically significant. Including substrate type in the regression increased predictive power to 68% (SE = 2.27°C) in the case of RMs (Table S2a) and 92% (SE = 1.49°C) for RLs (Table S2b). If biomimetic temperatures are assumed to be representative of living organisms (see Sections 2.2 and 5), this implies that under the same exposure conditions, substrate type contributes to differences in the peak temperatures of common rocky shore organisms. Similar results were found in the (wet) laboratory simulations, with surface $T_{max\text{-}air}$ alone explaining 64% (SE = 2.14°C) of the variation in RM peaks ($R^2 = 0.64$, $F[1,22] = 38.67$, $p < 0.001$) compared to 82% (SE = 2.66°C) for RLs ($R^2 = 0.82$, $F[1,22] = 100.07$, $p < 0.001$). Including substrate type in

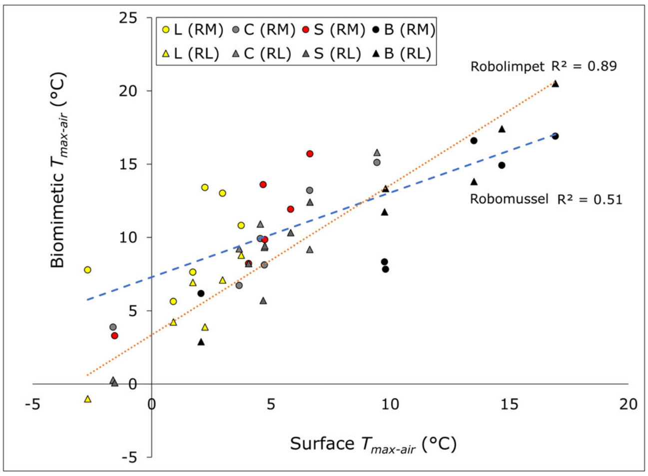

FIGURE 6 Maximum recorded temperatures above peak air temperature ($T_{\text{max-air}}$) of two biomimetic sensors (robomussels [RMs], circles; robolimpets [RLs], triangles) attached to four substrates (limestone [L], yellow; concrete [C], grey; sandstone [S], red; basalt [B], black) across six different field exposures in southern England (Table 2). Negative values indicate instances when the surfaces of L, S and C (and the RMs attached to L and S) peaked below maximum air temperature on an overcast day. Regression lines for RMs and RLs are shown.

the regressions of the simulation data increased the predictive power of the RM model to 71% (SE = 1.86°C; Table S3a) but did not improve the RL model (Table S3b). This reflects the already highly significant predictive power of surface temperature alone for RLs in the laboratory simulations. The strong relationship between substrate type and surface temperature in the simulations (see Section 4.1) also gave rise to moderate collinearity effects (based on *VIF* values) in the RM model (Table S3a), meaning that their individual contributions to logger temperatures could not be determined with confidence.

The relatively strong relationship between surface and RL $T_{\text{max-air}}$ reflects their greater degree of contact, conducive to more efficient conductive heat transfer from substrate to organism (Seuront, Ng, & Lathlean, 2018; Wethey, 2002). This mimics the attachment of living limpets, whose body tissues are in direct contact with the substrates, unlike mussels (Miller & Denny, 2011). This suggests that divergent thermal behaviours of different substrates in a warming climate are of particular significance for these organisms. For example, in the field, a 1°C increase in surface $T_{\text{max-air}}$ corresponded to an average 1.0°C increase in RL $T_{\text{max-air}}$ compared to only 0.6°C for RMs (Figure 6). Thermal exchanges (from substrate to organism in this case) are mediated by rock properties such as thermal conductivity, which determines the rate at which heat conducts through and away from the surface (Cryan et al., 2021). Thus, relative to other rock types, the high thermal conductivity of basalt, which always attained the highest peak temperatures, is conducive to greater transfers of heat to attached organisms. Supporting this, in Figure 6, clusters of the same-coloured points indicate that the sensors attached to the progressively hotter limestone, sandstone, concrete and basalt also generally attained higher peak temperatures. At the same time, the trends in Figure 6 also reflect variations in insolation intensity across the different exposure days and, therefore, differences in the direct solar heating of the sensors, although this could not be measured in the field.

The stronger link between surface and RL temperatures was also observed in the laboratory simulations, but there was a notable inconsistency in the relative temperatures of the two sensors; RLs tended to record higher $T_{\text{max-air}}$ values in the laboratory whereas RMs were consistently hotter in the field, at least on the substrates other than basalt (compare field data in Figure 6 with simulation data in Figure 7). This may reflect more efficient heating of RMs in the field, as higher solar zenith angles (i.e. heating from the side) resulted in the RM 'shells' receiving more incident insolation compared to the flatter RLs (Seuront, Ng, & Lathlean, 2018). The opposite was true in the laboratory, where direct heating from above meant that incident radiation occurred over a greater surface area of the RLs relative to the RMs. The dark colour of the RMs may also have contributed to their higher T_{max} values in the field (Mitton, 1977), although such relationships are not always clear for rocky shore organisms (Cox & Smith, 2011). It is also interesting that in contrast to the cooler substrates, the RLs attached to basalt peaked higher than their adjacent RMs in four out of five clear-sky days in the field. This further indicates the relative importance of conductive heat transfers to organisms attached to thermally responsive substrates like basalt.

4.3 | Substrate evaporative cooling mediates surface and biomimetic temperatures

4.3.1 | Dry versus wet simulations

Based on precisely replicated laboratory simulations, the overall trend was for higher peak biomimetic temperatures on hotter surfaces (Figure 7), mirroring the field data. Compared to the dry simulations (Figure 7a), both surface and biomimetic $T_{\text{max-air}}$ were reduced under the wet state in all cases (Figure 7b). For the different substrates, the magnitudes of this 'cooling' effect matched the variation in porosities (Table 1). Thus, the surface $T_{\text{max-air}}$ of wet sandstone (porosity = 19%) was reduced by an average of 8.6 ± 1.2°C, that of limestone (porosity = 18%) by 5.8 ± 2.1°C, that of concrete (porosity = 12%) by 3.5 ± 2.1°C and that of basalt (porosity = 1%) by 2.3 ± 1.3°C. Gravimetric changes before and after the wet simulations (see Table S4) confirmed the differences in evaporative losses, with higher-porosity substrates losing more water by weight and, simultaneously, contributing to lower peak temperatures relative to air. The dispersion and overlap of the $T_{\text{max-air}}$ data points across the different substrates are also greater for the wet simulations (Figure 7), indicating that moisture and associated evaporative effects amplified the thermal divergence between the substrates and the sensors attached to them. The differences in colour between wet and dry surfaces may also have contributed to this (Table 1).

Given that the specific heat capacity of water is approximately five times higher than that of rock, substrate water content is expected to have a dominating influence on overall specific heat capacity (Schärli & Rybach, 2001). Based on the results of this study, higher-porosity materials absorbing and holding more water during tidal immersion can subsequently lose more via evaporation during emersion, which in the field will depend on the time of day, weather conditions, tidal position and so forth. As a source of latent heat, evaporative cooling via water loss from epiliths is known to be an important thermoregulatory mechanism in the intertidal zone (e.g. Lathlean et al., 2016; Mitchell et al., 2024; also see Section 5); the laboratory observations show that evaporative cooling of intertidal substrates also influences rock-surface and organism thermal

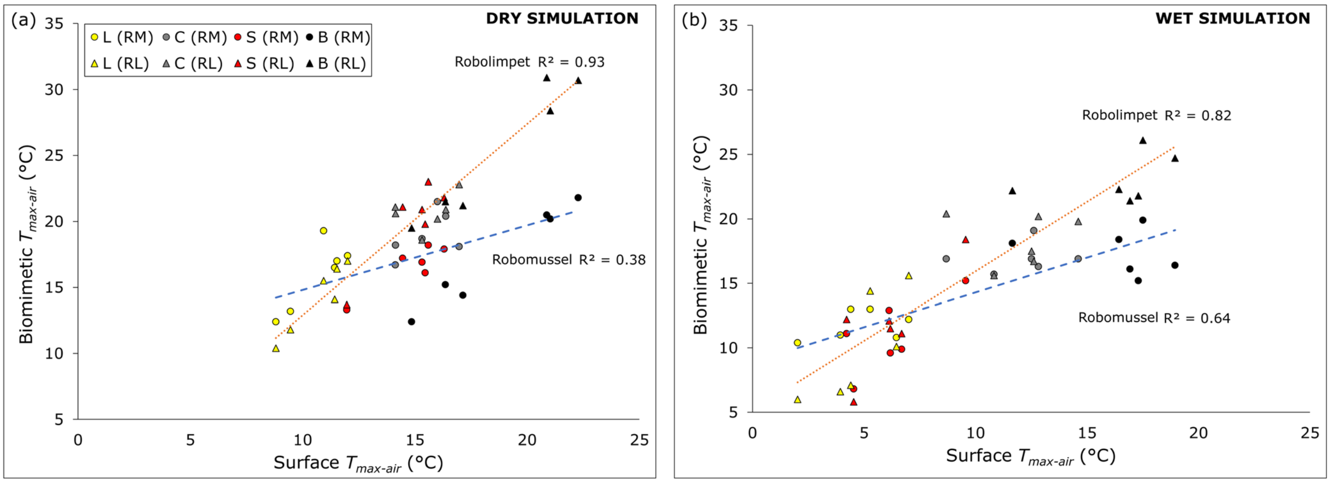

FIGURE 7 Relationships between surface and biomimetic peak temperatures relative to air ($T_{max-air}$) with (a) dry and (b) wet substrate blocks. Data points are for robomussels (RMs, circles) and robolimpets (RLs, triangles) attached to four substrates (limestone [L], yellow; concrete [C], grey; sandstone [S], red; basalt [B], black). The shift towards lower $T_{max-air}$ in Figure 7b reflects evaporative cooling influences alongside higher RH, and higher dispersion indicates amplification of substrate thermal properties under the wet condition.

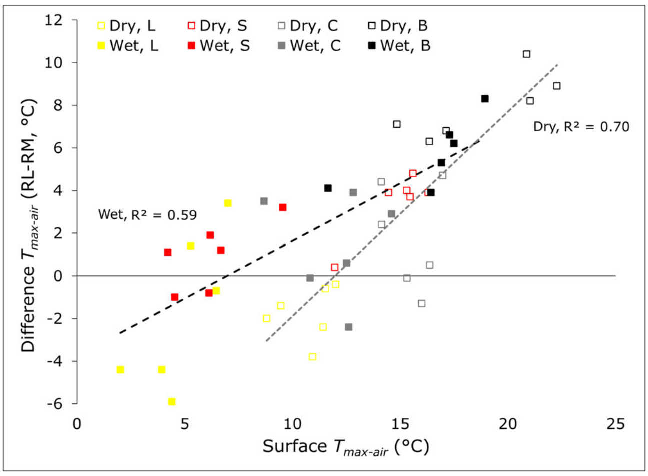

FIGURE 8 Differences between peak temperatures ($T_{max-air}$) of robolimpets (RLs) and robomussels (RMs) in dry (open fill) and wet (solid fill) laboratory simulations when attached to different substrates under the same heating conditions (yellow = limestone, L; red = sandstone, S; grey = concrete, C; black = basalt, B). Simulations were conducted across three scenarios (air temperature = 20, 30 or 40°C), each replicated twice in the dry and wet states. Positive values along the *y*-axis indicate that RLs attained relatively higher peak temperatures than RMs, and vice versa.

dynamics. These relationships are not easily observed in the field, but the kinds of replicated simulations reported here allow for carefully controlled comparisons between substrates and heating regimes, offering significant potential for further novel experimentation.

4.3.2 | RMs versus RLs

In addition to influencing thermal divergence between the substrates (Section 4.3.1), moisture also mediated thermal divergence between the two types of sensor. As shown in Figure 8, the overall trend was for greater differences in RL and RM $T_{max-air}$ (RL–RM) when the sensors were attached to hotter substrates, with RLs tending to peak higher than RMs overall (positive values in Figure 8). The regression lines in Figure 8 are for the dry (open fill) and wet (solid fill) simulations, respectively, when all other experimental variables were carefully controlled. Thus, differences in the data spread and the strength and slope of the regression lines are attributable primarily to the addition of moisture (both evaporative and RH effects in the chamber). When the substrates were dry, a 1°C increase in surface $T_{max-air}$ was associated with an equivalent 0.96°C increase in the difference between the sensor types (difference [dry] = $-11.49 + 0.96$(surface $T_{max-air}$); $R^2 = 0.70$, $F[1,22] = 51.00$, $p < 0.001$). When attached to wet substrates, this difference dropped to 0.54°C (difference [wet] = $-3.76 + 0.54$(surface $T_{max-air}$); $R^2 = 0.59$, $F[1,22] = 31.56$, $p < 0.001$).

These results show that evaporative cooling—the magnitude of which is at least partly determined by substrate porosity—mediated a divergence in peak biomimetic temperatures indicative of two common rocky shore organisms. This is attributed, at least in part, to the differing contact and thermal exchange with the substrate, as described in Section 4.2. Thus, while RLs are more responsive to diverging substrate temperatures, RMs probably lose heat more efficiently via convection (owing to greater protrusion into the boundary layer) as well as radiation under hotter conditions linked to organism shape and colour (Harley et al., 2009; Helmuth, 2002; Judge, Choi, & Helmuth, 2018; Mitchell et al., 2018). In this way, the type and physical properties of biological substrates linked to evaporation (i.e. porosity) influence surface and organism temperatures. This is supported by Table 4, in which the cooling effect of moisture and evaporation is quantified as the $T_{max-air}$ difference between the dry and wet simulations; in all scenarios, the magnitude of this cooling corresponded well to the relative porosities of the different substrates (S > L > C > B).

Table 4 also shows that the increase in evaporative cooling between the 20 and 30°C simulations was marked and positive for all substrates, whereas, except for basalt, additional warming to 40°C weakened this cooling effect slightly. This may reflect faster evaporation rates during the hottest scenario, meaning that the substrates

TABLE 4 Peak surface temperatures of substrates above air ($T_{\text{max-air}}$) when exposed under the same heating conditions (20, 30 or 40°C). Simulations were replicated under dry (dry blocks) and wet (saturated blocks) conditions. The differences ('diff.') between the wet and dry situations indicate the evaporative cooling effect. All values are the mean of two replicate simulations.

	20°C			30°C			40°C		
Air (fixed)	**Dry**	**Wet**	**Diff.**	**Dry**	**Wet**	**Diff.**	**Dry**	**Wet**	**Diff.**
Limestone	s10.20	6.73	−3.47	11.72	4.61	−7.11	10.17	3.21	−6.96
Sandstone	15.38	8.12	−7.26	15.53	6.16	−9.37	13.64	4.37	−9.27
Concrete	14.73	13.61	−1.12	16.68	11.82	−4.86	15.07	10.60	−4.47
Basalt	19.32	18.12	−1.20	19.01	16.97	−2.04	17.94	14.29	−3.65

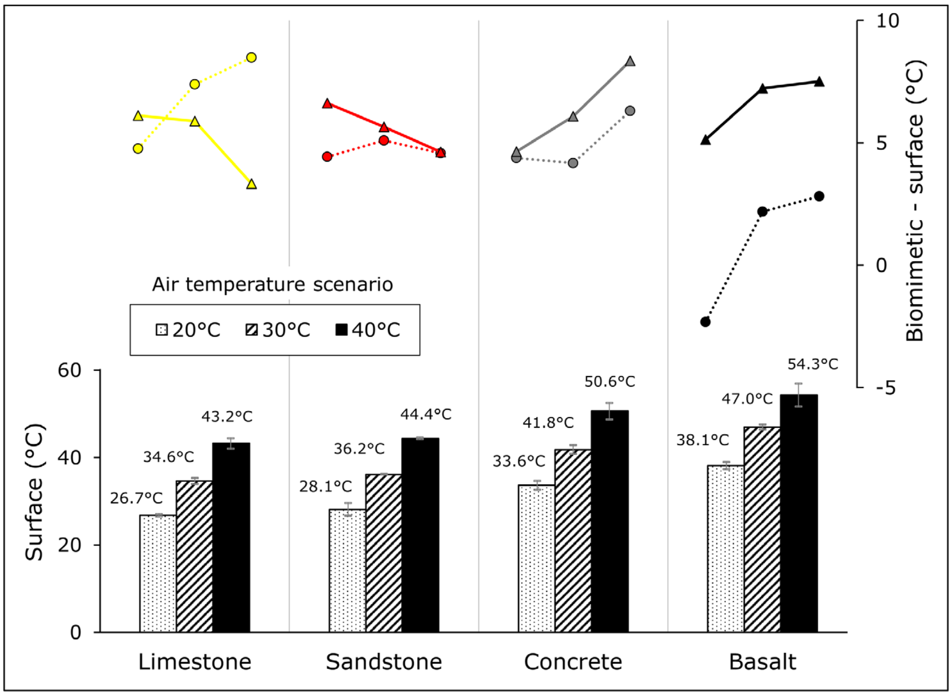

FIGURE 9 Surface thermal maxima ($T_{\max}$, $n = 2$) of four different substrates under three (wet) simulated heatwave scenarios (air = 20, 30 and 40°C) with corresponding biomimetic peaks relative to the surface (circles = robomussels, triangles = robolimpets).

dried more quickly and, therefore, moisture had less of an influence on $T_{\max}$ recorded at the end of the simulations. This effect would have been less influential for basalt, which, given its very low porosity, dried very quickly in all scenarios. The heat-mitigating effects of substrate evaporative cooling for attached organisms are, therefore, probably nonlinear, limited by rates of surface drying as controlled by water supply (as a function of porosity), the duration of exposure and heating (as a function of tidal position), and the temperature and RH of air (as a function of season and climate).

4.4 | Substrate type mediated thermal responses under increasingly extreme heatwave scenarios

Replicating the laboratory simulations at three different temperatures (20, 30 and 40°C) allowed comparisons under increasingly extreme but representative heatwave conditions in a way that was not possible in the field. As shown in Figure 9 (lower graph), based on the wet simulations, the relative increase in surface $T_{\max}$ across the three scenarios was consistent; the average increase between the 20 and 30°C scenarios was 8.2 ± 0.4°C compared to 8.2 ± 0.6°C between the 30 and 40°C scenarios. The relative differences between the substrates observed in the field (Figure 4) were also maintained, with limestone $T_{\max}$ < sandstone $T_{\max}$ < concrete $T_{\max}$ < basalt $T_{\max}$ under all three scenarios.

Despite this consistency in relative surface temperatures, interesting divergence was observed between the sensors across the three scenarios (Figure 9, upper graph). The overall trend for RMs was to attain similar or higher $T_{\text{max-air}}$ values with each 10°C increase in air temperature (dashed lines). In comparison, while the RLs attached to concrete and basalt also recorded higher relative values with each increase in air temperature, the opposite was true for those attached to limestone and sandstone, which showed successively lower $T_{\text{max-air}}$ (solid lines). This contrast for RLs likely further reflects the evaporative cooling effects described in Section 4.3. Specifically, relative to surface temperature, the sensors attached to the substrates that lost the most water during each simulation (sandstone and limestone) had progressively lower $T_{\text{max-air}}$ values as air temperature increased (Figure 9 and Supporting Information). This implies that compared to low-porosity rocks, porous substrates able to sustain evaporative cooling during exposure can moderate (reduce) the thermal maxima of those organisms attached to them. Crucially, the simulation data indicate that this relative cooling effect might be enhanced under increasingly extreme conditions, presumably because evaporation is more efficient under hotter conditions. The upper limits of these effects and their importance relative to other factors remain unknown.

The other notable difference in Figure 9 is the contrast between the sensor types attached to basalt, with RMs peaking an average of 5.7°C below RLs. This included the RMs remaining cooler than the basalt surface under the 20°C scenario (negative values in the figure), which was not observed for any other substrate. The reasons for such differences on this substrate are not clear but might indicate the modulation of radiative cooling of dark-coloured RMs when attached to the hot basalt. Further experiments with a greater level of replication will help address this in the future.

4.5 | Implications for thermal biology in a warming climate

Mortality resulting from the passing of critical physiological temperatures on rocky shores is a threshold-driven process (Miller & Denny, 2011; Smale & Wernberg, 2013). The factors influencing whether such critical limits are exceeded, including substrate effects, therefore have relevance in the context of thermal biology and climate change. As Seuront, Ng and Lathlean (2018) note, heat transfer from the substrate via conduction is an important determinant of epilith body temperature during intertidal exposure. Denny and Harley (2006) also make the point that colour contrasts between organisms (limpets in their case) and rock facilitate substantial transfers of heat between them. In the case when a lighter coloured and more thermally reflective limpet is attached to a darker and more thermally absorptive rock, such as basalt, conductive heat transfer from substrate to organism dominates, whereas the opposite might be true when attached to lighter surfaces. Along with other critical thermal properties such as specific heat capacity, this provides a plausible mechanism to explain why the sensors attached to the darker substrates generally attained higher $T_{\max}$ values, and vice versa, especially in the case of RLs.

Thermal differences between substrates are especially important when extreme temperatures occur during key life-history stages, such as larval settlement (Findlay et al., 2010). For example, the post-settlement survival of larvae on rocks that become relatively hot at low tide (e.g. basalt) may be lower compared to those that stay cooler (e.g. limestone and sandstone) (Raimondi, 1988; Tan et al., 2023). Kordas et al. (2015) provide direct evidence of this using black and white settlement plates in the Salish Sea. They attributed poor survival of barnacles, a relative absence of herbivores, and a decline in species richness on the black plates to their 2.6°C hotter surfaces on average relative to the white plates, although these effects did vary seasonally and spatially on the shore. In the current study, differences in peak temperatures between the substrates always exceeded this 2.6°C average (Figure 4), implying that thermal differences between shores composed of contrasting rocks could give rise to similar organism- and community-level outcomes. In addition to differences in surface temperature, the results of this study show that the relative porosities and drying rates of substrates could have similar ecological effects by worsening or mitigating desiccation stress (Lathlean, Ayre, & Minchinton, 2013; Miller, Harley, & Denny, 2009). The additional complexities of drying (and wetting) coupled with dynamic changes in surface colour and associated thermal properties and transfers—as were particularly marked for basalt and sandstone—remain to be fully examined in these contexts.

Although absolute critical thresholds are difficult to define owing to variations in individual organisms and patterns of exposure to heat (e.g. frequency, duration, pre-exposure conditions and so forth), lethal limits of various intertidal species have been determined in the laboratory and field (e.g. Miller, 2022; Miller, Harley, & Denny, 2009). Compared to the reported critical thermal limits of *Mytilus edulis* (25–37°C, Jones, Mieszkowska, & Wethey, 2009), biomimetic $T_{\max}$ values were within or surpassed this range during all field exposures and laboratory simulations, irrespective of substrate type. Caution is expressed, however, in directly equating these sensor values with the body temperatures of living organisms (see Section 5), as they most likely represent upper extremes. Nevertheless, given that the peak temperatures of the sensors consistently differed by several degrees or more, limpets and mussels will likely experience greater thermal extremes on shores composed of ‘hot rocks’ like basalt. These substrate effects might translate to differences in the spatial arrangement of individuals (Chapperon & Seuront, 2011) as well as regime shifts and altered ecological interactions (Hawkins, Bohn, & Doncaster, 2015; Meunier, Hacker, & Menge, 2024). The vulnerability of different genera to physiological stress when exposed to the same heating conditions was also demonstrated in this study, with those more closely attached to their substrates (RLs) attaining higher thermal peaks as a result of more efficient heat exchange. This effect has relevance for varying levels of heat stress experienced by different organisms attached on the same substrate or between the same organisms living on shores composed of different rocks.

In addition to its relevance for natural rocky shores, there is some evidence that material type impacts ecological communities on urbanised coasts via thermal effects alongside topographic and water-retaining influences (Aguilera, Arias, & Manzur, 2019). There is very little research, however, in this area relative to the growth in studies on the ecological functioning and enhancement of artificial coastal structures (e.g. Firth et al., 2024; Kosová et al., 2023). The inclusion of concrete in this study indicates such influences might be important. Future research in this area could inform options for thermal refuge provision through, for example, the careful selection and placement of ‘cool’ substrates within engineering schemes (Bauer et al., 2025; Coombes & Naylor, 2012; Lima et al., 2016; MacArthur et al., 2020).

Finally, in thermal biology, evaporative cooling has mainly been considered in the context of water loss from body tissues of organisms rather than from the substrate (e.g. Seuront, Ng, & Lathlean, 2018). Interestingly, Denny and Harley (2006) suggest that evaporative cooling was not important in predicting limpet body temperatures using a thermal model based on the high accuracy of their predictions when excluding this as a variable. They did, however, use granite, a non-porous material, in their modelling, whereas the wet and dry simulations using materials with a range of porosities reported here indicate that evaporation could have some effect on relevant metrics (i.e. thermal maxima). This, in turn, was found to moderate biomimetic peak temperatures to some extent (Figures 7 and 8). These observations emphasise the importance of substrate physical properties alongside type when comparing and predicting thermal conditions and ecological responses across space and time. Importantly, the influences of synergistic thermal and evaporative processes on surface temperatures were found to vary considerably between substrate types, warranting greater attention in thermal biology studies.

5 | FUTURE RESEARCH DIRECTIONS FOR THERMAL BIOGEOMORPHOLOGY ON ROCKY SHORES

Manipulative field experiments and controlled laboratory studies are valuable approaches to studying complex environmental systems. Relating findings to real-world conditions does, however, present several challenges (e.g. Smith et al., 2005). Building on this work as a proof-of-concept study, the following five research directions are highlighted: First, the impacts of substrate sample size and physical characteristics as used in experiments need further assessment. Rock size influences thermal stress responses in colonising marine organisms (Gedan et al., 2011), meaning there is a trade-off between using smaller, practical samples in experiments versus data collection on larger in situ rock masses, for which key properties such as thermal inertia can be very different. Such scale challenges are well recognised when using sample blocks and laboratory observations in geomorphological research (Moses, 2000; Smith et al., 2005; Viles, 2001). Using flat, cut surfaces was a crucial part of the experimental design, enabling standardised comparisons, but this simplifies the complex reality of thermal transfers among the ocean, air, organisms and rock (e.g. Lathlean et al., 2014). For example, differences in heating angles explained some conflicting results between the field and laboratory datasets (Section 4.2). The influences of these and other substrate factors on the kinds of thermal differences reported here, including different scales of surface complexity, could be explored in future research, building on thermal biology studies by combining laboratory, field and modelling approaches (Judge, Choi, & Helmuth, 2018; Seuront, Ng, & Lathlean, 2018; Tan et al., 2023).

Second, the representativeness of biomimetic sensors needs further consideration in thermal biogeomorphological research. Despite recording data more representative of living organisms than standard measures of temperature, biomimetic sensors cannot replicate behavioural thermoregulatory responses under heat stress (Judge, Choi, & Helmuth, 2018; Seuront, Ng, & Lathlean, 2018). In intertidal molluscs such as limpets and mussels, these responses include actively seeking refuge, ‘mushrooming’, ‘shell-lifting’ and ‘gaping’ behaviours (Masanja et al., 2023; Miller & Denny, 2011; Williams et al., 2005), all of which can significantly reduce body temperatures (Helmuth, 1999). This limits the direct comparability of temperatures recorded using biomimetic sensors with those experienced by living organisms, although their value relative to standard loggers and for comparative studies is clear. As is emphasised in thermal biology research (e.g. Miller & Dowd, 2017), the integration of field and modelling datasets of living organisms to supplement sensor-based experiments is also needed in thermal biogeomorphology research.

Third, community-scale influences remain a significant gap in biogeomorphological understanding. While individual sensors were used in this study to allow standardised comparisons, limpets and mussels occur as aggregations of individuals, particularly in the case of mussels, which often form dense beds of hundreds to thousands of individuals. These aggregations influence thermal conditions through (1) shading effects, (2) water retention and (3) concurrent radiation/conduction of heat among individuals and with the air and substrate. Such aggregations create cooler microhabitats and mitigate temperature extremes (Baxter, Coombes, & Viles, 2022; Chapperon & Seuront, 2011; Miller & Dowd, 2017; Olabarria et al., 2016). Dense organic covers also modulate substrate heating and cooling by shading and holding water at the surface (Coombes et al., 2017; Gonzalez et al., 2021). In addition, the thermal buffering effects of foundation species such as canopy-forming seaweeds are critical ecosystem engineering processes on rocky shores (Gutiérrez et al., 2011; Harley, 2006; Hesketh & Harley, 2023). There is, therefore, a need to explore such bi-directional thermal interactions between aggregations and communities of individuals and their substrates, including the likely spatio-temporally dynamic effects of variable organic cover (e.g. Coombes et al., 2013; Viles et al., 2008).

Fourth, the complexity introduced by multiple environmental variables across space and time requires more investigation. Larger-scale environmental factors play a significant role in thermal dynamics on rocky shores but were necessarily simplified in this study. This includes shore position, timing and duration of tidal exposure, antecedent weather conditions, and water retention on the surface (Lathlean & Seuront, 2014; Lathlean, Seuront, & Ng, 2017; Tan et al., 2023). Topographic complexity at scales ranging from centimetres to metres (Hesketh & Harley, 2023) and from metres to several kilometres (Lathlean & McQuaid, 2017) also influence the occurrence of critical temperatures and outcomes at the patch-to-regional scale. The influences of these controls relative to (and in combination with) substratum type remain unknown. In addition to well-replicated field exposure studies deploying different substrates in the same locations, the growing networks of temperature loggers in the coastal zone (including the Coupled Temperature and Biodiversity Observation Network; see Reese, 2023) offer opportunities for rock–substratum thermal studies in combination with other factors across a broad range of scales.

Lastly, the implications of the kinds of processes and relationships discussed here need to be considered in the contexts of biogeomorphological feedbacks and dynamics. While this research has focussed on the contributions of rocky substrates and physical properties to thermal biology, the relationships discussed have wider biogeomorphological relevance that warrant further attention. For example, thermal stresses and mortality under heatwave conditions, as shown here to be mediated by substrate hygro-thermal behaviours, lead to shifts in the distribution and abundance of species across a range of scales (e.g. Mieszkowska et al., 2021). This will likely involve shifts in the occurrence of geomorphologically relevant species, including the occurrence and activity of bioeroders (e.g. grazing limpets) and bioprotectors (e.g. mussels as well as canopy-forming algae) both on natural rocky shores and artificial structures (Baxter, Coombes, & Viles, 2022; Coombes et al., 2013, 2017; Cooper et al., 2025). The sensitivity of these different organisms to thermal shifts, the changes in the efficacy of their geomorphic work, and the spatial scales and timeframes over which such effects might play out all require specific attention by biogeomorphologists in collaboration with thermal biologists and ecological modellers.

6 | CONCLUSIONS

The results of this study show that alongside the diversity of other factors influencing complex thermal dynamics on rocky shores, substrate type and physical properties can mediate—if not modulate—the temperatures recorded by biomimetic sensors. These data are indicative of divergent surface temperatures even when heating conditions are controlled for. Regression analysis showed that peak biomimetic temperatures were best explained when substrate type was considered, and the divergent thermal responses of different sensors (RLs and RMs) were linked to their degree of surface attachment and, consequently, conductive thermal exchange.

These findings indicate that spatially and temporally divergent physiological stresses in rocky shore organisms are likely influenced by substrate type and key physical properties, including porosity and its association with evaporative cooling of the substrate. A key remaining challenge is determining the significance of these effects relative to other substrate, organism and environmental factors that influence the thermal landscape of rocky shores across a range of scales. Nevertheless, given that substrate temperatures diverged by many degrees under hot summertime and heatwave conditions, rock type and thermal properties could determine whether critical thermal limits are crossed. In addition to their implications for ecological communities and biodiversity, these effects may also mediate shifts in the abundance and distribution of geomorphologically relative species on rocky shores. Going forward, a greater integration of approaches and techniques from biogeomorphology and thermal biology will help improve our understanding of the complex bi-directional thermal interactions and outcomes on rocky shores—offering opportunities for a new thermal biogeomorphology. This is critical for explaining and predicting spatially and temporally variable ecological and linked biogeomorphological responses in a warming and more extreme climate.

AUTHOR CONTRIBUTIONS

MAC conceived and designed the study, acquired the funding, conducted the data collection and analyses, and wrote the original and revised manuscript.

ACKNOWLEDGEMENTS

I am hugely grateful to Prof. Heather Viles for her support and stimulating discussions on many aspects of this work. I also thank A. Townsend and Nellie for fieldwork support.

CONFLICT OF INTEREST STATEMENT

I have no conflict of interest to disclose.

DATA AVAILABILITY STATEMENT

All original data used in this study are deposited in the Oxford Research Archive (ORA), available at https://ora.ox.ac.uk/objects/uuid_cbdfc0ca-01ec-48e5-8f31-f21d1df19802.

REFERENCES

Aguilera, M.A., Arias, R.M. & Manzur, T. (2019) Mapping microhabitat thermal patterns in artificial breakwaters: alteration of intertidal biodiversity by higher rock temperature. *Ecology and Evolution*, 9(22), 12915–12927. Available from: https://doi.org/10.1002/ece3.5776

Bauer, F., Knights, A.M., Hanley, M.E., Griffin, J.N., Foggo, A., Brown, A., et al. (2025) Thermal patterns on eco-engineered coastal infrastructure depend on topographic complexity and spatial scale. *Ecological Engineering*, 215, 107596. Available from: https://doi.org/10.1016/j.ecoleng.2025.107596

Baxter, T.I., Coombes, M.A. & Viles, H.A. (2022) The bioprotective properties of the blue mussel (Mytilus edulis) on intertidal rocky shore platforms. *Marine Geology*, 445, 106734. Available from: https://doi.org/10.1016/j.margeo.2022.106734

Beukema, J.J., Dekker, R. & Jansen, J.M. (2009) Some like it cold: populations of the tellinid bivalve Macoma balthica (L.) suffer in various ways from a warming climate. *Marine Ecology Progress Series*, 384, 135–145. Available from: https://doi.org/10.3354/meps07952

Bowker, D., Davis, R., Myrick, D., Stacy, E., & Jones, W. (1985) Spectral reflectance of natural targets for use in remote sensing studies. NASA Reference Publication 1139; 182.

Capotondi, A., Rodrigues, R.R., Sen Gupta, A., Benthuysen, J.A., Deser, C., Frölicher, T.L., et al. (2024) A global overview of marine heatwaves in a changing climate. *Communications Earth & Environment*, 5(1), 701. Available from: https://doi.org/10.1038/s43247-024-01806-9

Chan, B.K.K., Lima, F.P., Williams, G.A., Seabra, R. & Wang, H.-Y. (2016) A simplified biomimetic temperature logger for recording intertidal barnacle body temperatures. *Limnology and Oceanography: Methods*, 14(7), 448–455. Available from: https://doi.org/10.1002/lom3.10103

Chapperon, C. & Seuront, L. (2011) Space–time variability in environmental thermal properties and snail thermoregulatory behaviour. *Functional Ecology*, 25(5), 1040–1050. Available from: https://doi.org/10.1111/j.1365-2435.2011.01859.x

Coombes, M.A. (2011) Rock warming and drying under simulated intertidal conditions, part I: experimental procedures and comparisons with field data. *Earth Surface Processes and Landforms*, 36(15), 2114–2121. Available from: https://doi.org/10.1002/esp.2230

Coombes, M.A. (2014) The rock coast of the British Isles: weathering and biogenic processes. In: Kennedy, D.M., Stephenson, W.J. & Naylor, L.A. (Eds.) *Rock coast geomorphology: a global synthesis*, Vol. 40. Geological Society, London, Memoirs, pp. 57–76 https://doi.org/10.1144/m40.5

Coombes, M.A. & Naylor, L.A. (2012) Rock warming and drying under simulated intertidal conditions, part II: weathering and biological influences on evaporative cooling and near-surface micro-climatic conditions as an example of biogeomorphic ecosystem engineering. *Earth Surface Processes and Landforms*, 37(1), 100–118. Available from: https://doi.org/10.1002/esp.2232

Coombes, M.A., Naylor, L.A., Viles, H.A. & Thompson, R.C. (2013) Bioprotection and disturbance: seaweed, microclimatic stability and conditions for mechanical weathering in the intertidal zone. *Geomorphology*, 202, 4–14. Available from: https://doi.org/10.1016/j.geomorph.2012.09.014

Coombes, M.A., Viles, H.A., Naylor, L.A. & La Marca, E.C. (2017) Cool barnacles: do common biogenic structures enhance or retard rates of deterioration of intertidal rocks and concrete? *Science of the Total Environment*, 580, 1034–1045. Available from: https://doi.org/10.1016/j.scitotenv.2016.12.058

Cooper, A., Knights, A.M., Walker, S., Sempere-Valverde, J., Moocarme, C., Hawkins, S.J., et al. (2025) The role of limpets in biodiversity patterns and bioerosion on coastal infrastructure: insights from Plymouth Breakwater. *Ecological Engineering*, 213, 107548. Available from: https://doi.org/10.1016/j.ecoleng.2025.107548

Cox, T.E. & Smith, C.M. (2011) Thermal ecology on an exposed algal reef: infrared imagery a rapid tool to survey temperature at local spatial scales. *Coral Reefs*, 30(4), 1109–1120. Available from: https://doi.org/10.1007/s00338-011-0799-2

Cryan, A., Choi, F., Adams, D. & Helmuth, B. (2021) Heat budget model facilitates exploration of thermal ecology on urban shoreline infrastructure. *Ecological Engineering*, 171, 106371. Available from: https://doi.org/10.1016/j.ecoleng.2021.106371

Davison, I.R. & Pearson, G.A. (1996) Stress tolerance in intertidal seaweeds. *Journal of Phycology*, 32(2), 197–211. Available from: https://doi.org/10.1111/j.0022-3646.1996.00197.x

Denny, M.W. & Harley, C.D.G. (2006) Hot limpets: predicting body temperature in a conductance-mediated thermal system. *Journal of Experimental Biology*, 209(13), 2409–2419. Available from: https://doi.org/10.1242/jeb.02257

Denny, M.W., Miller, L.P. & Harley, C.D.G. (2006) Thermal stress on intertidal limpets: long-term hindcasts and lethal limits. *Journal of*

Experimental Biology, 209(13), 2420–2431. Available from: https://doi.org/10.1242/jeb.02258

Dong, Y.-W. (2023) Roles of multi-level temperature-adaptive responses and microhabitat variation in establishing distributions of intertidal species. *Journal of Experimental Biology*, 226(21), 245745. Available from: https://doi.org/10.1242/jeb.245745

Findlay, H.S., Kendall, M.A., Spicer, J.I. & Widdicombe, S. (2010) Post-larval development of two intertidal barnacles at elevated CO2 and temperature. *Marine Biology*, 157(4), 725–735. Available from: https://doi.org/10.1007/s00227-009-1356-1

Finke, G.R., Navarrete, S.A. & Bozinovic, F. (2007) Tidal regimes of temperate coasts and their influences on aerial exposure for intertidal organisms. *Marine Ecology Progress Series*, 343, 57–62. Available from: https://doi.org/10.3354/meps06918

Firth, L.B., Bone, J., Bartholomew, A., Bishop, M.J., Bugnot, A., Bulleri, F., et al. (2024) Coastal greening of grey infrastructure: an update on the state of the art. *Proceedings of the Institution of Civil Engineers: Maritime Engineering*, 177, 35–67. Available from: https://doi.org/10.1680/jmaen.2023.003

Garrabou, J., Coma, R., Bensoussan, N., Bally, M., ChevaldonnÉ, P., Cigliano, M., et al. (2009) Mass mortality in northwestern Mediterranean rocky benthic communities: effects of the 2003 heat wave. *Global Change Biology*, 15(5), 1090–1103. Available from: https://doi.org/10.1111/j.1365-2486.2008.01823.x

Gedan, K.B., Bernhardt, J., Bertness, M.D. & Leslie, H.M. (2011) Substrate size mediates thermal stress in the rocky intertidal. *Ecology*, 92(3), 576–582. Available from: https://doi.org/10.1890/10-0717.1

Gonzalez, J.A., Coombes, M.A., Palomo, M.G., Isla, F.I., Soria, S.A. & Gutiérrez, J.L. (2021) Enhanced weathering and erosion of a cohesive shore platform following the experimental removal of mussels. *Frontiers in Marine Science*, 8, 756016. Available from: https://doi.org/10.3389/fmars.2021.756016

Gowell, M.R., Coombes, M.A. & Viles, H.A. (2015) Rock-protecting seaweed? Experimental evidence of bioprotection in the intertidal zone. *Earth Surface Processes and Landforms*, 40(10), 1364–1370. Available from: https://doi.org/10.1002/esp.3736

Gutiérrez, J.L., Jones, C.G., Byers, J.E., Arkema, K.K., Berkenbusch, K., Commito, J.A., et al. (2011) 7.04 - physical ecosystem engineers and the functioning of estuaries and coasts. In: *Treatise on estuarine and coastal science*. Waltham: Academic Press, pp. 53–81 https://doi.org/10.1016/B978-0-12-374711-2.00705-1

Hall, K. & Thorn, C.E. (2014) Thermal fatigue and thermal shock in bedrock: an attempt to unravel the geomorphic processes and products. *Geomorphology*, 206, 1–13. Available from: https://doi.org/10.1016/j.geomorph.2013.09.022

Harley, C.D.G. (2006) Effects of physical ecosystem engineering and herbivory on intertidal community structure. *Marine Ecology Progress Series*, 317, 29–39. Available from: https://doi.org/10.3354/meps317029

Harley, C.D.G. (2008) Tidal dynamics, topographic orientation, and temperature-mediated mass mortalities on rocky shores. *Marine Ecology Progress Series*, 371, 37–46. Available from: https://doi.org/10.3354/meps07711

Harley, C.D.G., Denny, M.W., Mach, K.J. & Miller, L.P. (2009) Thermal stress and morphological adaptations in limpets. *Functional Ecology*, 23(2), 292–301. Available from: https://doi.org/10.1111/j.1365-2435.2008.01496.x

Harley, C.D.G. & Helmuth, B.S.T. (2003) Local- and regional-scale effects of wave exposure, thermal stress, and absolute versus effective shore level on patterns of intertidal zonation. *Limnology and Oceanography*, 48(4), 1498–1508. Available from: https://doi.org/10.4319/lo.2003.48.4.1498

Harley, C.D.G., Randall Hughes, A., Hultgren, K.M., Miner, B.G., Sorte, C.J.B., Thornber, C.S., et al. (2006) The impacts of climate change in coastal marine systems. *Ecology Letters*, 9(2), 228–241. Available from: https://doi.org/10.1111/j.1461-0248.2005.00871.x

Hawkins, S.J., Burrows, M.T. & Mieszkowska, N. (2023) Shoreline sentinels of global change show the consequences of extreme events. *Global Change Biology*, 29(1), 7–9. Available from: https://doi.org/10.1111/gcb.16477

Hawkins, S.J., Bohn, K. & Doncaster, C.P. (2015) Ecosystems: the rocky road to regime-shift indicators. *Current Biology*, 25(15), R666–R669. Available from: https://doi.org/10.1016/j.cub.2015.06.027

Helmuth, B. (1998) Intertidal mussel microclimates: predicting the body temperature of a sessile invertebrate. *Ecological Monographs*, 68(1), 51–74. Available from: https://doi.org/10.1890/0012-9615(1998)068[0051:IMMPTB]2.0.CO;2

Helmuth, B. (1999) Thermal biology of rocky intertidal mussels: quantifying body temperatures using climatological data. *Ecology*, 80(1), 15–34. Available from: https://doi.org/10.1890/0012-9658(1999)080[0015:TBORIM]2.0.CO;2

Helmuth, B. (2002) How do we measure the environment? Linking intertidal thermal physiology and ecology through biophysics. *Integrative and Comparative Biology*, 42(4), 837–845. Available from: https://doi.org/10.1093/icb/42.4.837

Helmuth, B., Choi, F., Matzelle, A., Torossian, J.L., Morello, S.L., Mislan, K.A.S., et al. (2016) Long-term, high frequency in situ measurements of intertidal mussel bed temperatures using biomimetic sensors. *Nature Scientific Data*, 3(1), 160087. Available from: https://doi.org/10.1038/sdata.2016.87

Helmuth, B., Mieszkowska, N., Moore, P. & Hawkins, S.J. (2006) Living on the edge of two changing worlds: forecasting the responses of rocky intertidal ecosystems to climate change. *Annual Review of Ecology, Evolution, and Systematics*, 37(1), 373–404. Available from: https://doi.org/10.1146/annurev.ecolsys.37.091305.110149

Hesketh, A.V. & Harley, C.D.G. (2023) Extreme heatwave drives topography-dependent patterns of mortality in a bed-forming intertidal barnacle, with implications for associated community structure. *Global Change Biology*, 29(1), 165–178. Available from: https://doi.org/10.1111/gcb.16390

Hobday, A.J., Alexander, L.V., Perkins, S.E., Smale, D.A., Straub, S.C., Oliver, E.C.J., et al. (2016) A hierarchical approach to defining marine heatwaves. *Progress in Oceanography*, 141, 227–238. Available from: https://doi.org/10.1016/j.pocean.2015.12.014

Hobday, A.J., Burrows, M.T., Filbee-Dexter, K., Holbrook, N.J., Sen Gupta, A., Smale, D.A., et al. (2023) With the arrival of El Niño, prepare for stronger marine heatwaves. *Nature*, 621(7977), 38–41. Available from: https://doi.org/10.1038/d41586-023-02730-2

Ishida, K., Tachibana, M., Yao, Y., Wada, Y. & Noda, T. (2023) The impact of marine heatwaves on rocky intertidal communities: evidence of accumulative carryover effects of marine heatwaves. *Frontiers in Marine Science*, 10, 1146148. Available from: https://doi.org/10.3389/fmars.2023.1146148

Janetzki, N., Benkendorff, K. & Fairweather, P.G. (2021) Rocks of different mineralogy show different temperature characteristics: implications for biodiversity on rocky seashores. *PeerJ*, 9, e10712. Available from: https://doi.org/10.7717/peerj.10712

Jones, S.J., Mieszkowska, N. & Wethey, D.S. (2009) Linking thermal tolerances and biogeography: Mytilus edulis (L.) at its southern limit on the East Coast of the United States. *Biological Bulletin*, 217(1), 73–85. Available from: https://doi.org/10.1086/BBLv217n1p73

Judge, M.L., Botton, M.L. & Hamilton, M.G. (2011) Physiological consequences of the supralittoral fringe: microhabitat temperature profiles and stress protein levels in the tropical periwinkle Cenchritis muricatus (Linneaus, 1758). *Hydrobiologia*, 675(1), 143–156. Available from: https://doi.org/10.1007/s10750-011-0812-3

Judge, R., Choi, F. & Helmuth, B. (2018) Recent advances in data logging for intertidal ecology. *Frontiers in Ecology and Evolution*, 6, 00213. Available from: https://doi.org/10.3389/fevo.2018.00213

Kearney, M., Simpson, S.J., Raubenheimer, D. & Helmuth, B. (2010) Modelling the ecological niche from functional traits. *Philosophical Transactions of the Royal Society, B: Biological Sciences*, 365(1557), 3469–3483. Available from: https://doi.org/10.1098/rstb.2010.0034

Kendon, M. (2023) Heatwave, September 2023. Met Office National Climate Information Centre. https://www.metoffice.gov.uk/binaries/content/assets/metofficegovuk/pdf/weather/learn-about/uk-past-events/interesting/2023/2023_05_september_heatwave.pdf Accessed 03 January 2025.

Kennedy, D.M., Stephenson, W.J. & Naylor, L.A. (2014) Introduction to the rock coasts of the world. In: Kennedy, D.M., Stephenson, W.J. &

Naylor, L.A. (Eds.) *Rock coast geomorphology: a global synthesis*, Vol. 40. Geological Society, London, Memoirs, pp. 1–5 https://doi.org/10.1144/m40.1

King, N.G., Leathers, T., Smith, K.E. & Smale, D.A. (2025) The influence of pre-exposure to marine heatwaves on the critical thermal maxima (CT) of marine foundation species. *Functional Ecology*, 39(8), 1869–1878. Available from: https://doi.org/10.1111/1365-2435.14622

Kordas, R.L., Dudgeon, S., Storey, S. & Harley, C.D.G. (2015) Intertidal community responses to field-based experimental warming. *Oikos*, 124(7), 888–898. Available from: https://doi.org/10.1111/oik.00806

Kosová, E., James, K., MacArthur, M., Vovides, A., Peters, J., Metcalfe, D., et al. (2023) The BioGeo Ecotile: improving biodiversity on coastal defences using a multiscale, multispecies eco-engineering design. *Ecological Engineering*, 188, 106881. Available from: https://doi.org/10.1016/j.ecoleng.2022.106881

Lathlean, J. & Seuront, L. (2014) Infrared thermography in marine ecology: methods, previous applications and future challenges. *Marine Ecology Progress Series*, 514, 263–277. Available from: https://doi.org/10.3354/meps10995

Lathlean, J.A., Ayre, D.J., Coleman, R.A. & Minchinton, T.E. (2014) Using biomimetic loggers to measure interspecific and microhabitat variation in body temperatures of rocky intertidal invertebrates. *Marine and Freshwater Research*, 66(1), 86–94. Available from: https://doi.org/10.1071/MF13287

Lathlean, J.A., Ayre, D.J. & Minchinton, T.E. (2013) Temperature variability at the larval scale affects early survival and growth of an intertidal barnacle. *Marine Ecology Progress Series*, 475, 155–166. Available from: https://doi.org/10.3354/meps10105

Lathlean, J.A. & McQuaid, C.D. (2017) Biogeographic variability in the value of mussel beds as ecosystem engineers on south African rocky shores. *Ecosystems*, 20(3), 568–582. Available from: https://doi.org/10.1007/s10021-016-0041-8

Lathlean, J.A., McWilliam, R.A., Pankhurst, J. & Minchinton, T.E. (2017) Altering species interactions outweighs the effects of experimental warming in structuring a rocky shore community. *Journal of Experimental Marine Biology and Ecology*, 496, 22–28. Available from: https://doi.org/10.1016/j.jembe.2017.08.001

Lathlean, J.A., Seuront, L., McQuaid, C.D., Ng, T.P.T., Zardi, G.I. & Nicastro, K.R. (2016) Size and position (sometimes) matter: small-scale patterns of heat stress associated with two co-occurring mussels with different thermoregulatory behaviour. *Marine Biology*, 163(9), 189. Available from: https://doi.org/10.1007/s00227-016-2966-z

Lathlean, J.A., Seuront, L. & Ng, T.P.T. (2017) On the edge: the use of infrared thermography in monitoring responses of intertidal organisms to heat stress. *Ecological Indicators*, 81, 567–577. Available from: https://doi.org/10.1016/j.ecolind.2017.04.057

Lima, F.P., Gomes, F., Seabra, R., Wethey, D.S., Seabra, M.I., Cruz, T., et al. (2016) Loss of thermal refugia near equatorial range limits. *Global Change Biology*, 22(1), 254–263. Available from: https://doi.org/10.1111/gcb.13115

Lima, F.P. & Wethey, D.S. (2009) Robolimpets: measuring intertidal body temperatures using biomimetic loggers. *Limnology and Oceanography: Methods*, 7(5), 347–353. Available from: https://doi.org/10.4319/lom.2009.7.347

MacArthur, M., Naylor, L.A., Hansom, J.D. & Burrows, M.T. (2020) Ecological enhancement of coastal engineering structures: passive enhancement techniques. *Science of the Total Environment*, 740, 139981. Available from: https://doi.org/10.1016/j.scitotenv.2020.139981

Marshall, D.J., McQuaid, C.D. & Williams, G.A. (2010) Non-climatic thermal adaptation: implications for species' responses to climate warming. *Biology Letters*, 6(5), 669–673. Available from: https://doi.org/10.1098/rsbl.2010.0233

Masanja, F., Yang, K., Xu, Y., He, G., Liu, X., Xu, X., et al. (2023) Impacts of marine heat extremes on bivalves. *Frontiers in Marine Science*, 10, 1159261. Available from: https://doi.org/10.3389/fmars.2023.1159261

McGreevy, J.P. (1985) Thermal properties as controls on rock surface temperature maxima, and possible implications for rock weathering. *Earth Surface Processes and Landforms*, 10(2), 125–136. Available from: https://doi.org/10.1002/esp.3290100205

Meager, J.J., Schlacher, T.A. & Green, M. (2011) Topographic complexity and landscape temperature patterns create a dynamic habitat structure on a rocky intertidal shore. *Marine Ecology Progress Series*, 428, 1–12. Available from: https://doi.org/10.3354/meps09124

Meunier, Z.D., Hacker, S.D. & Menge, B.A. (2024) Regime shifts in rocky intertidal communities associated with a marine heatwave and disease outbreak. *Nature Ecology & Evolution*, 8(7), 1285–1297. Available from: https://doi.org/10.1038/s41559-024-02425-5

Mieszkowska, N., Burrows, M.T., Hawkins, S.J. & Sugden, H. (2021) Impacts of pervasive climate change and extreme events on rocky intertidal communities: evidence from long-term data. *Frontiers in Marine Science*, 8, 642764. Available from: https://doi.org/10.3389/fmars.2021.642764

Miller, L.P. (2022) Monitoring bivalve behavior and physiology in the laboratory and field using open-source tools. *Integrative and Comparative Biology*, 62(4), 1096–1110. Available from: https://doi.org/10.1093/icb/icac046

Miller, L.P. & Denny, M.W. (2011) Importance of behavior and morphological traits for controlling body temperature in Littorinid snails. *The Biological Bulletin*, 220(3), 209–223. Available from: https://doi.org/10.1086/BBLv220n3p209

Miller, L.P. & Dowd, W.W. (2017) Multimodal in situ datalogging quantifies inter-individual variation in thermal experience and persistent origin effects on gaping behavior among intertidal mussels (Mytilus californianus). *The Journal of Experimental Biology*, 220(Pt 22), 4305–4319. Available from: https://doi.org/10.1242/jeb.164020

Miller, L.P., Harley, C.D.G. & Denny, M.W. (2009) The role of temperature and desiccation stress in limiting the local-scale distribution of the owl limpet, Lottia gigantea. *Functional Ecology*, 23(4), 756–767. Available from: https://doi.org/10.1111/j.1365-2435.2009.01567.x

Mislan, K.A.S., Wethey, D.S. & Helmuth, B. (2009) When to worry about the weather: role of tidal cycle in determining patterns of risk in intertidal ecosystems. *Global Change Biology*, 15(12), 3056–3065. Available from: https://doi.org/10.1111/j.1365-2486.2009.01936.x

Mitchell, D., Maloney, S.K., Snelling, E.P., Carvalho Fonsêca, V.F. & Fuller, A. (2024) Measurement of microclimates in a warming world: problems and solutions. *Journal of Experimental Biology*, 227(13), jeb246481. Available from: https://doi.org/10.1242/jeb.246481

Mitchell, D., Snelling, E.P., Hetem, R.S., Maloney, S.K., Strauss, W.M. & Fuller, A. (2018) Revisiting concepts of thermal physiology: predicting responses of mammals to climate change. *Journal of Animal Ecology*, 87(4), 956–973. Available from: https://doi.org/10.1111/1365-2656.12818

Mitton, J.B. (1977) Shell color and pattern variation in Mytilus edulis and its adaptive significance. *Chesapeake Science*, 18(4), 387–390. Available from: https://doi.org/10.2307/1350595

Moses, C.A. (2000) Field rock block exposure trials. *Zeitschrift für Geomorphologie*, 120, 33–50.

Mottershead, D. (2013) Coastal weathering. In: Shroder, J.F. (Ed.) *Treatise on geomorphology*. San Diego: Academic Press, pp. 228–244 https://doi.org/10.1016/B978-0-12-374739-6.00064-6

Naylor, L.A., Coombes, M.A. & Viles, H.A. (2012) Reconceptualising the role of organisms in the erosion of rock coasts: a new model. *Geomorphology*, 157-158, 17–30. Available from: https://doi.org/10.1016/j.geomorph.2011.07.015

Naylor, L.A., Viles, H.A. & Carter, N.E.A. (2002) Biogeomorphology revisited: looking towards the future. *Geomorphology*, 47(1), 3–14. Available from: https://doi.org/10.1016/S0169-555X(02)00137-X

Olabarria, C., Gestoso, I., Lima, F.P., Vázquez, E., Comeau, L.A., Gomes, F., et al. (2016) Response of two Mytilids to a heatwave: the complex interplay of physiology, behaviour and ecological interactions. *PLoS ONE*, 11(10), e0164330. Available from: https://doi.org/10.1371/journal.pone.0164330

Paine, R.T. & Levin, S.A. (1981) Intertidal landscapes: disturbance and the dynamics of pattern. *Ecological Monographs*, 51(2), 145–178. Available from: https://doi.org/10.2307/2937261

Pearson, G.A., Lago-Leston, A. & Mota, C. (2009) Frayed at the edges: selective pressure and adaptive response to abiotic stressors are mismatched in low diversity edge populations. *Journal of Ecology*, 97(3), 450–462. Available from: https://doi.org/10.1111/j.1365-2745.2009.01481.x

Petes, L.E., Menge, B.A. & Harris, A.L. (2008) Intertidal mussels exhibit energetic trade-offs between reproduction and stress resistance. *Ecological Monographs*, 78(3), 387–402. Available from: https://doi.org/10.1890/07-0605.1

Porter, W.P. & Gates, D.M. (1969) Thermodynamic equilibria of animals with environment. *Ecological Monographs*, 39(3), 227–244. Available from: https://doi.org/10.2307/1948545

Raimondi, P.T. (1988) Rock type affects settlement, recruitment, and zonation of the barnacle Chthamalus anisopoma Pilsbury. *Journal of Experimental Marine Biology and Ecology*, 123(3), 253–267. Available from: https://doi.org/10.1016/0022-0981(88)90046-9

Reese, A. (2023) Shore patrol. *Science*, 382(6670), 505–507. Available from: https://doi.org/10.1126/science.adl6586

Rejmánek, M. (1971) Ecological meaning of the thermal behaviour of rocks. *Flora*, 160(6), 527–561. Available from: https://doi.org/10.1016/S0367-2530(17)32040-6

Robinson, D.A. & Moses, C.A. (2011) Rock surface and weathering: process and form. In: Gregory, K.J. & Gouide, A.S. (Eds.) *The SAGE handbook of geomorphology*. London: SAGE, p. 291. Available from: https://doi.org/10.4135/9781446201053.n17

Sarà, G., Kearney, M. & Helmuth, B. (2011) Combining heat-transfer and energy budget models to predict thermal stress in Mediterranean intertidal mussels. *Chemistry and Ecology*, 27(2), 135–145. Available from: https://doi.org/10.1080/02757540.2011.552227

Schärli, U. & Rybach, L. (2001) Determination of specific heat capacity on rock fragments. *Geothermics*, 30(1), 93–110. Available from: https://doi.org/10.1016/S0375-6505(00)00035-3

Seuront, L., Ng, T.P.T. & Lathlean, J.A. (2018) A review of the thermal biology and ecology of molluscs, and of the use of infrared thermography in molluscan research. *Journal of Molluscan Studies*, 84(3), 203–232. Available from: https://doi.org/10.1093/mollus/eyy023

Seuront, L., Nicastro, K.R., Zardi, G.I. & Goberville, E. (2019) Decreased thermal tolerance under recurrent heat stress conditions explains summer mass mortality of the blue mussel Mytilus edulis. *Scientific Reports*, 9(1), 17498. Available from: https://doi.org/10.1038/s41598-019-53580-w

Smale, D.A. & Wernberg, T. (2013) Extreme climatic event drives range contraction of a habitat-forming species. *Proceedings of the Royal Society B: Biological Sciences*, 280(1754), 20122829. Available from: https://doi.org/10.1098/rspb.2012.2829

Smale, D.A., Wernberg, T., Oliver, E.C.J., Thomsen, M., Harvey, B.P., Straub, S.C., et al. (2019) Marine heatwaves threaten global biodiversity and the provision of ecosystem services. *Nature Climate Change*, 9(4), 306–312. Available from: https://doi.org/10.1038/s41558-019-0412-1

Smith, B.J. & McGreevy, J.P. (1983) A simulation study of salt weathering in hot deserts. *Geografiska Annaler: Series A, Physical Geography*, 65(1-2), 127–133. Available from: https://doi.org/10.1080/04353676.1983.11880079

Smith, B.J., Warke, P.A., McGreevy, J.P. & Kane, H.L. (2005) Salt-weathering simulations under hot desert conditions: agents of enlightenment or perpetuators of preconceptions? *Geomorphology*, 67(1-2), 211–227. Available from: https://doi.org/10.1016/j.geomorph.2004.03.015

Smith, K.E., Burrows, M.T., Hobday, A.J., Sen Gupta, A., Moore, P.J., Thomsen, M., et al. (2021) Socioeconomic impacts of marine heatwaves: global issues and opportunities. *Science*, 374(6566), eabj3593. Available from: https://doi.org/10.1126/science.abj3593

Somero, G.N. (2002) Thermal physiology and vertical zonation of intertidal animals: optima, limits, and costs of living1. *Integrative and Comparative Biology*, 42(4), 780–789. Available from: https://doi.org/10.1093/icb/42.4.780

Spencer, T. & Viles, H. (2002) Bioconstruction, bioerosion and disturbance on tropical coasts: coral reefs and rocky limestone shores. *Geomorphology*, 48(1-3), 23–50. Available from: https://doi.org/10.1016/S0169-555X(02)00174-5

Suits, D.B. (1957) Use of dummy variables in regression equations. *Journal of the American Statistical Association*, 52(280), 548–551. Available from: https://doi.org/10.1080/01621459.1957.10501412

Tan, Y., Sun, Y.-X., Zhu, Y.-J., Liao, M.-L. & Dong, Y.-W. (2023) The impacts of thermal heterogeneity across microhabitats on post-settlement selection of intertidal mussels. *iScience*, 26(12), 108376. Available from: https://doi.org/10.1016/j.isci.2023.108376

Trenhaile, A. (2014) Modelling the effect of Pliocene–quaternary changes in sea level on stable and tectonically active land masses. *Earth Surface Processes and Landforms*, 39, 1221–1235. Available from: https://doi.org/10.1002/esp.3574

Trudgill, S.T. (1987) Bioerosion of intertidal limestone, Co. Clare, Eire — 3: zonation, process and form. *Marine Geology*, 74, 111–121. Available from: https://doi.org/10.1016/0025-3227(87)90009-0

Tsuchiya, M. (1983) Mass mortality in a population of the mussel Mytilus edulis L. caused by high temperature on rocky shores. *Journal of Experimental Marine Biology and Ecology*, 66(2), 101–111. Available from: https://doi.org/10.1016/0022-0981(83)90032-1

Viles, H.A. (2001) Scale issues in weathering studies. *Geomorphology*, 41(1), 63–72. Available from: https://doi.org/10.1016/S0169-555X(01)00104-0

Viles, H.A. & Coombes, M.A. (2022) Biogeomorphology in the Anthropocene: a hierarchical, traits-based approach. *Geomorphology*, 417, 108446. Available from: https://doi.org/10.1016/j.geomorph.2022.108446

Viles, H.A., Naylor, L.A., Carter, N.E.A. & Chaput, D. (2008) Biogeomorphological disturbance regimes: progress in linking ecological and geomorphological systems. *Earth Surface Processes and Landforms*, 33(9), 1419–1435. Available from: https://doi.org/10.1002/esp.1717

Warke, P.A., Smith, B.J. & Magee, R.W. (1996) Thermal response characteristics of stone: implications for weathering of soiled surfaces in urban environments. *Earth Surface Processes and Landforms*, 21(3), 295–306. Available from: https://doi.org/10.1002/(SICI)1096-9837(199603)21:3%3C295::AID-ESP637%3E3.0.CO;2-8

Wernberg, T., Smale, D.A., Tuya, F., Thomsen, M.S., Langlois, T.J., de Bettignies, T., et al. (2013) An extreme climatic event alters marine ecosystem structure in a global biodiversity hotspot. *Nature Climate Change*, 3(1), 78–82. Available from: https://doi.org/10.1038/nclimate1627

Wethey, D.S. (2002) Biogeography, competition, and microclimate: the barnacle Chthamalus fragilis in New England1. *Integrative and Comparative Biology*, 42(4), 872–880. Available from: https://doi.org/10.1093/icb/42.4.872

Williams, G.A., De Pirro, M., Leung, K.M.Y. & Morritt, D. (2005) Physiological responses to heat stress on a tropical shore: the benefits of mushrooming behaviour in the limpet Cellana grata. *Marine Ecology Progress Series*, 292, 213–224. Available from: https://doi.org/10.3354/meps292213

Xiong, J., Lin, H., Ding, H., Pei, H., Rong, C. & Liao, W. (2020) Investigation on thermal property parameters characteristics of rocks and its influence factors. *Natural Gas Industry B*, 7(3), 298–308. Available from: https://doi.org/10.1016/j.ngib.2020.04.001

SUPPORTING INFORMATION

Additional supporting information can be found online in the Supporting Information section at the end of this article.

How to cite this article: Coombes, M.A. (2025) Hot rocks? Divergent rock-surface temperatures during extreme thermal events with implications for physiological stress in rocky shore organisms. *Earth Surface Processes and Landforms*, 50(13), e70182. Available from: https://doi.org/10.1002/esp.70182